

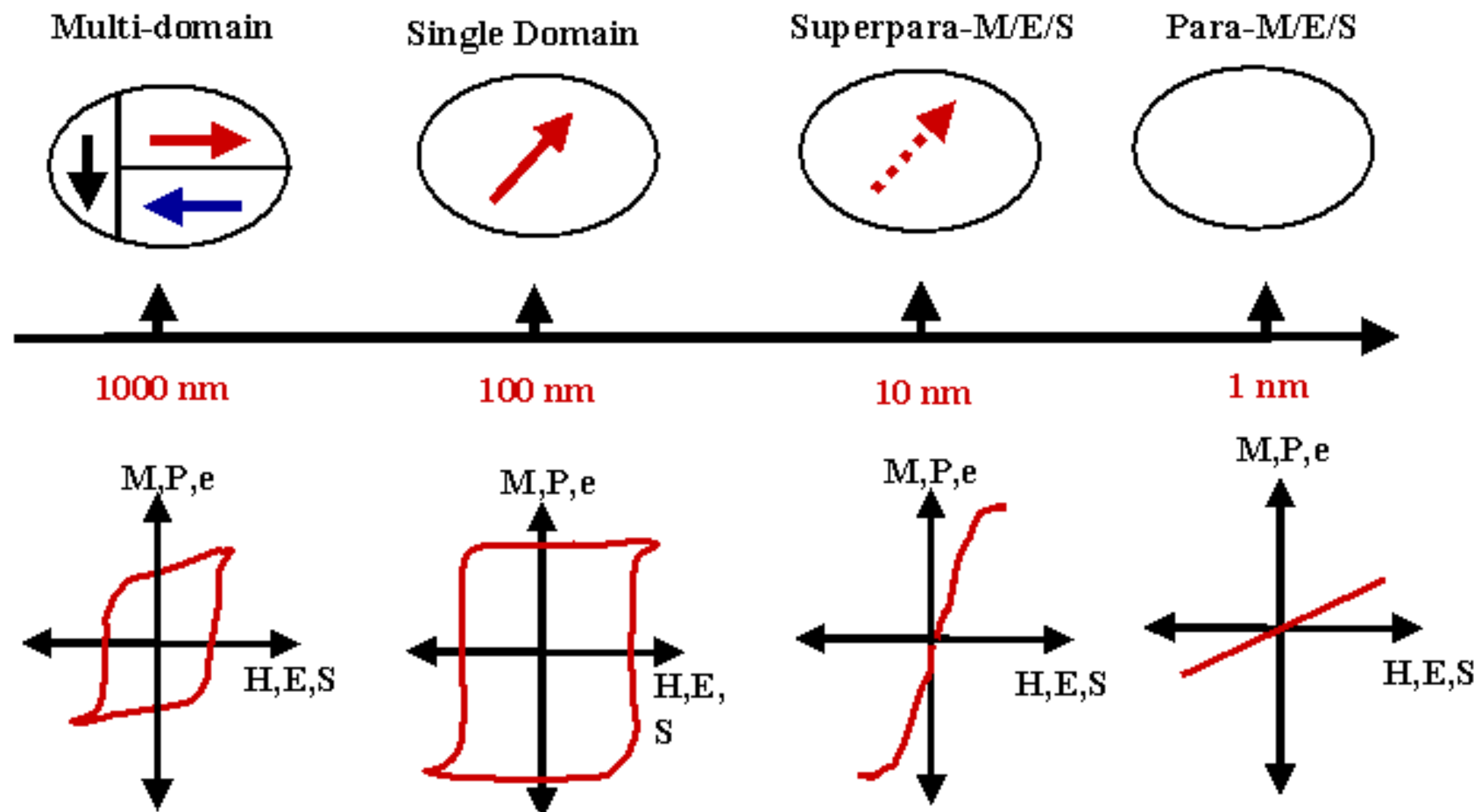
Ferroelectric and Ferromagnetic Nanoparticles for High Energy and Power Density Applications

Todd C. Monson, Chris B. Diantonio, Tom P.
Chavez, Jean L. Leger, Dale L. Huber

tmonson@sandia.gov

April, 2011

SIZE EFFECTS IN FERROICS (R. E. Newnham, 1992)



Transitions expected in *Ferromagnetics, Ferroelectrics and Ferroelastics* as a function of size.....

Ferroelectric Nanoparticles

Benefits of Nanocrystalline Dielectrics

Nanocrystalline ceramics show much higher breakdown strength (BDS) compared to coarse grain ceramics → higher energy density

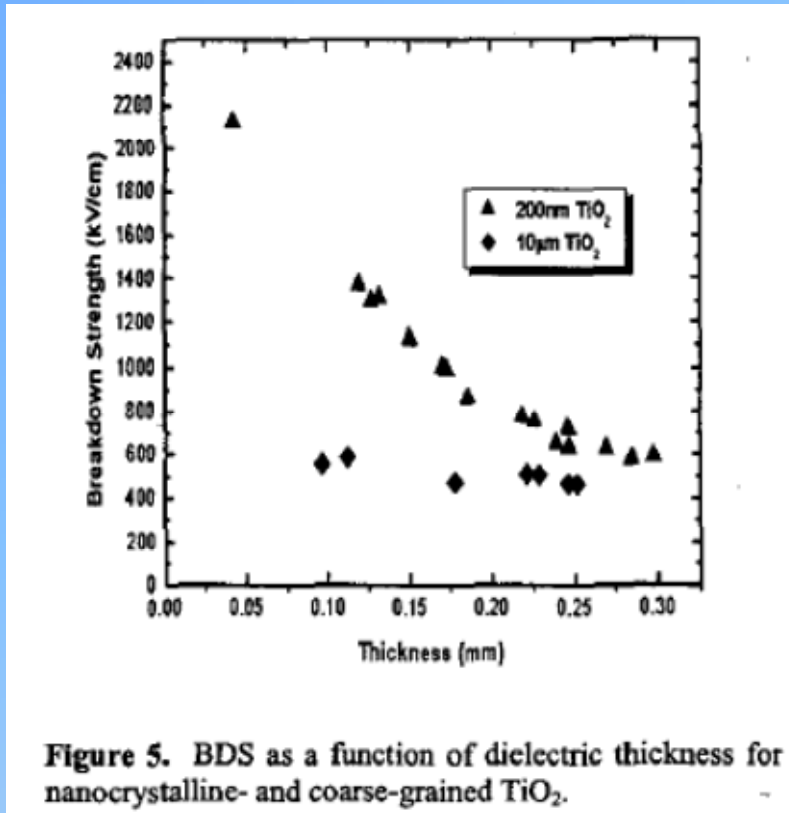


Figure 5. BDS as a function of dielectric thickness for nanocrystalline- and coarse-grained TiO_2 .

Ye et. al., "Influence of nanocrystalline grain size on the breakdown strength of ceramic dielectrics", 2003

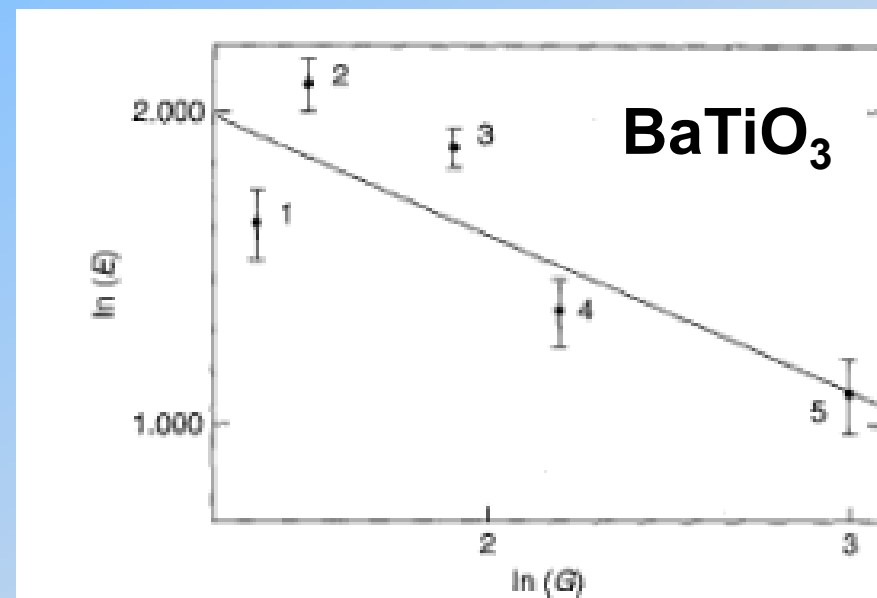


Figure 2. Grain size dependence on dielectric strength. Numbers indicate sintering temperatures: (1) 1320 °C, (2) 1330 °C, (3) 1350 °C, (4) 1380 °C, (5) 1400 °C.

Tunkasiri and Rujijanaul, J. Mater. Sci. Lett. 15 1767 (1996)

Benefits of Nanocrystalline Ferroelectrics

- For ferroelectric (FE) dielectrics, there are additional benefits:
 - Permittivity increases with decreasing grain size down to a critical size dimension (higher energy density)
 - High frequency performance improves with decreasing grain size (maintain permittivity and low loss to higher frequencies)
 - Field dependence of permittivity may improve (i.e. lower voltage coefficient of capacitance or VCC)

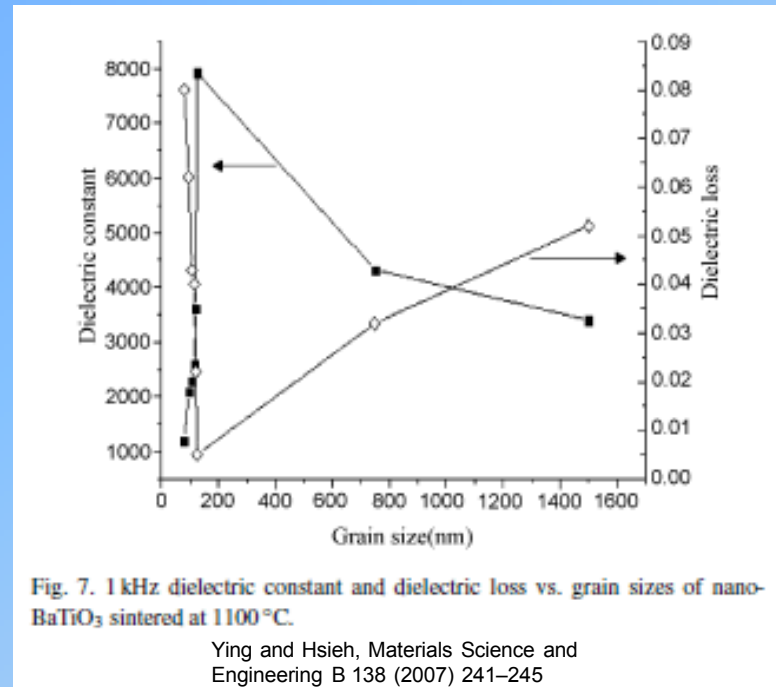


Fig. 7. 1 kHz dielectric constant and dielectric loss vs. grain sizes of nano- BaTiO_3 sintered at 1100 °C.

Ying and Hsieh, Materials Science and Engineering B 138 (2007) 241–245

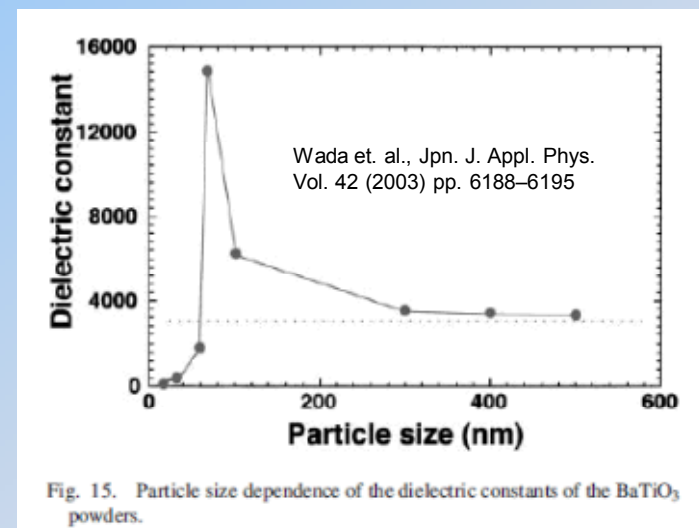


Fig. 15. Particle size dependence of the dielectric constants of the BaTiO_3 powders.

Benefits of Nanocrystalline Ferroelectrics

- Nano-scale grains lose long range ordering
- Reduce lattice coupling and hence reduce strain →
- Better electromechanical performance and increased shot life

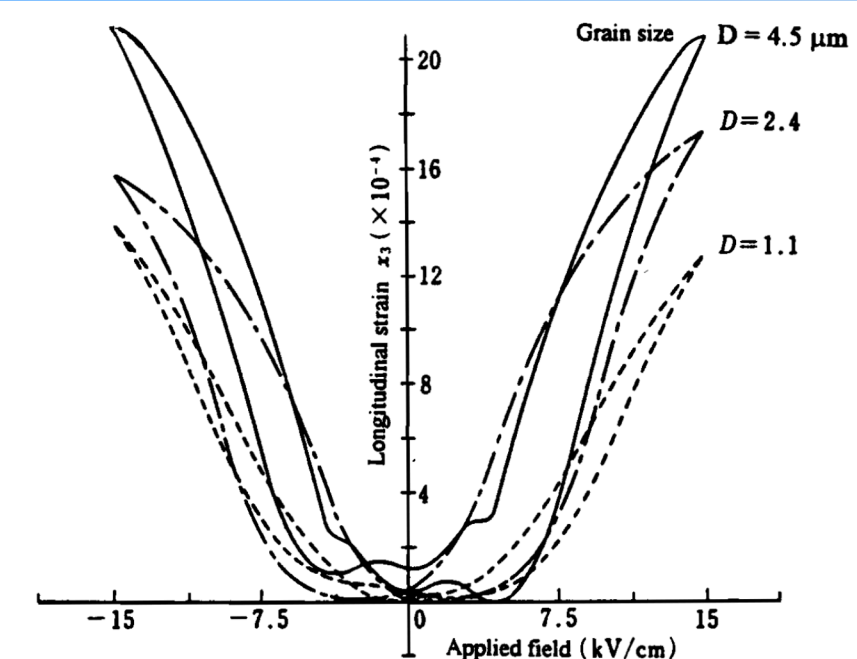
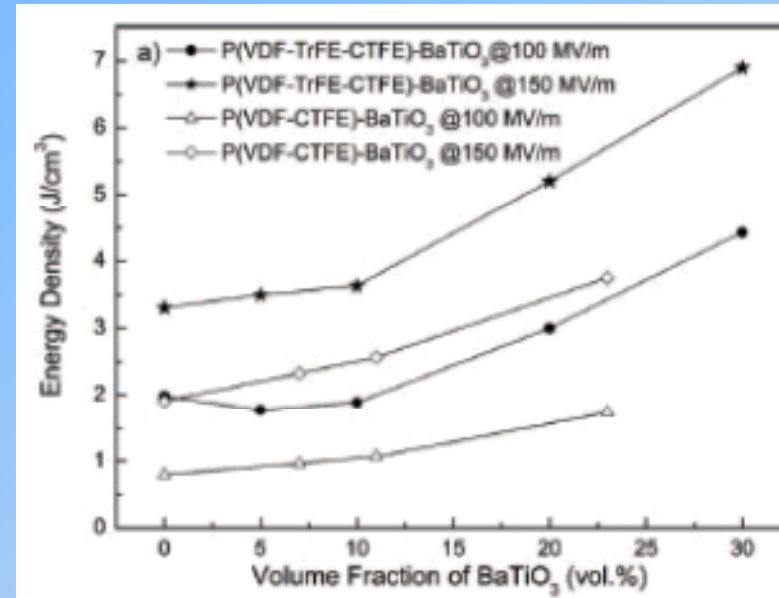
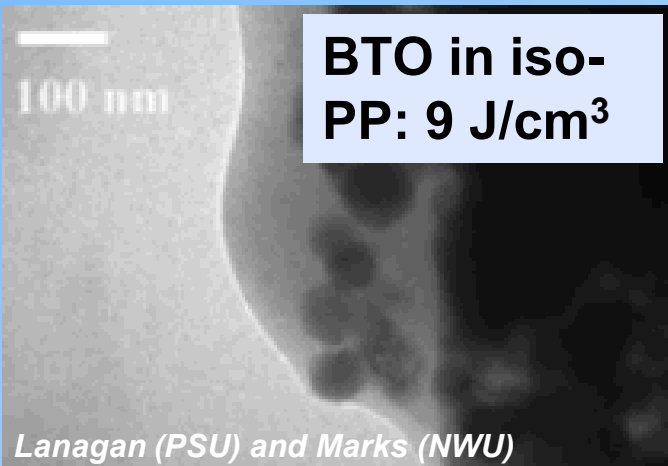
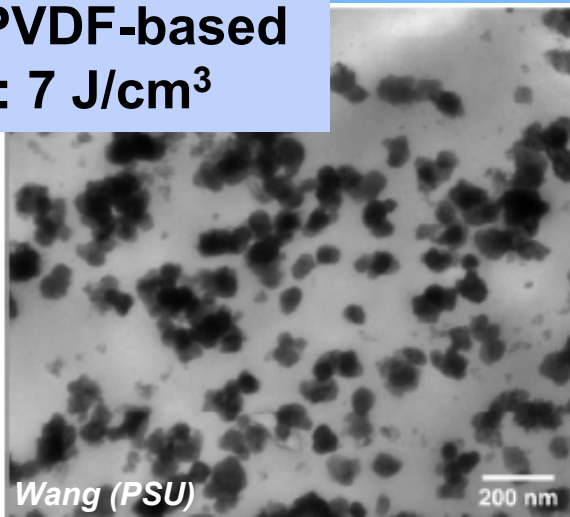


Fig. 3.28 Grain size dependence of the induced strain in PLZT ceramics.

from Kenji Uchino's book, Ferroelectric Devices

Polymer-Based Nanocomposite Dielectric Films

BTO in PVDF-based polymer: 7 J/cm³



- High energy densities demonstrated, but proof of performance in devices is lacking
- Low volumetric fraction of the inorganic particles (~ 25-30% loading)
- Size effects in ferroics not exploited

Ceramic/Glass Nanocomposite Solution

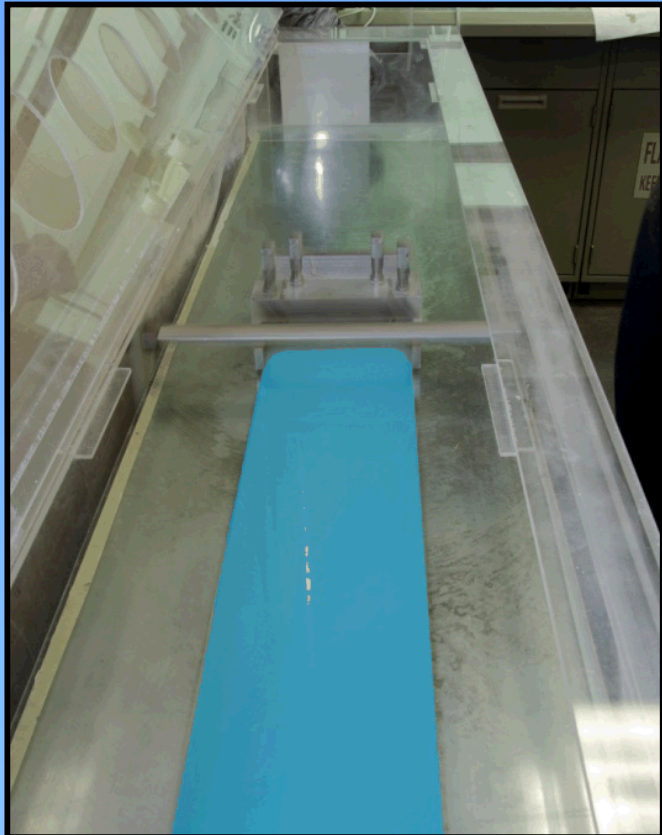
- Greater energy density through higher volumetric loading of the high permittivity dielectric
 - Glass based nanocomposite matrix provides a method for obtaining >90% loading of the nanoceramic → higher energy density

Volume mixing law: $\log \varepsilon = v_1 \times \log \varepsilon_1 + v_2 \times \log \varepsilon_2$

Energy Density: $EnergyDensity = \frac{1}{2} \varepsilon_0 \varepsilon_r E^2$

- Glass matrix should provide better thermal stability than polymer materials for improved TCC (Temperature Coefficient of Capacitance)
- Glass phase has been shown to improve electromechanical reliability (higher BDS & shot life)
 - Composite structure can support electric fields well in excess of 500 V/mil
- More robust devices

Integration into Multilayer Configuration



- The technology for fabricating multilayer polymer-based nanocomposite capacitors for pulsed energy applications is not mature
- This effort uses ceramic tape casting routes for casting, laminating, and firing multilayer parts

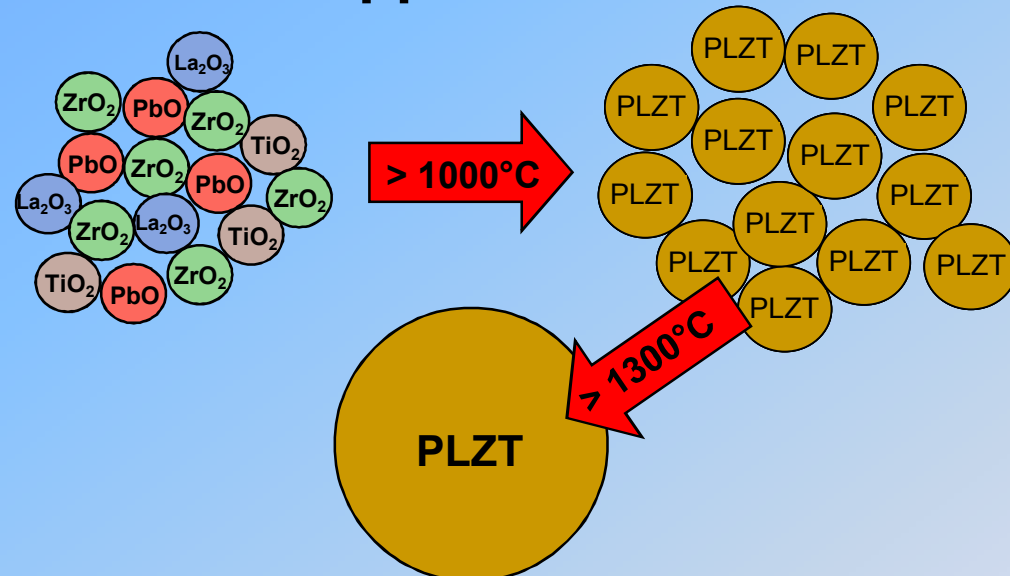
Lab-scale tape casting setup at SNL

Materials Approach

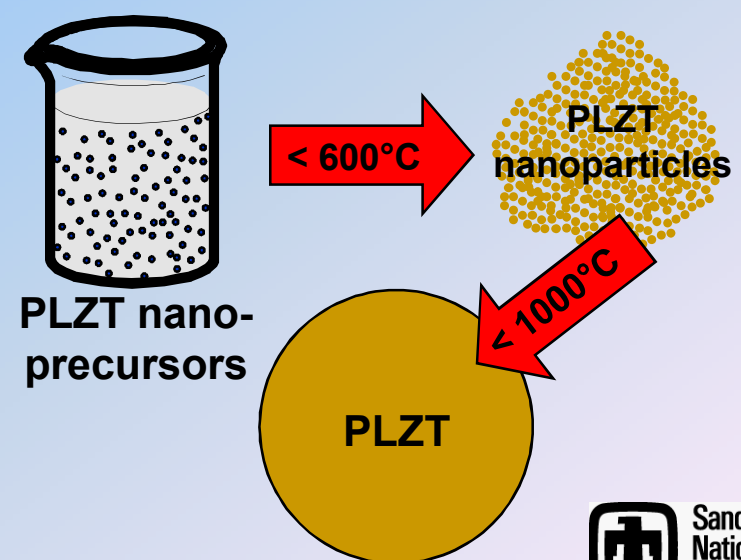
Approach:

- Synthesize nanoscale precursors for ceramic capacitors using room temperature solution based chemistry
- Develop sintering profile for nanoscale precursors and incorporate grain growth inhibitors and/or sintering aids to decrease firing temperature further and improve device performance

Traditional approach:



Our approach:



PLZT

PLZT Scaleable Aqueous Synthesis Route

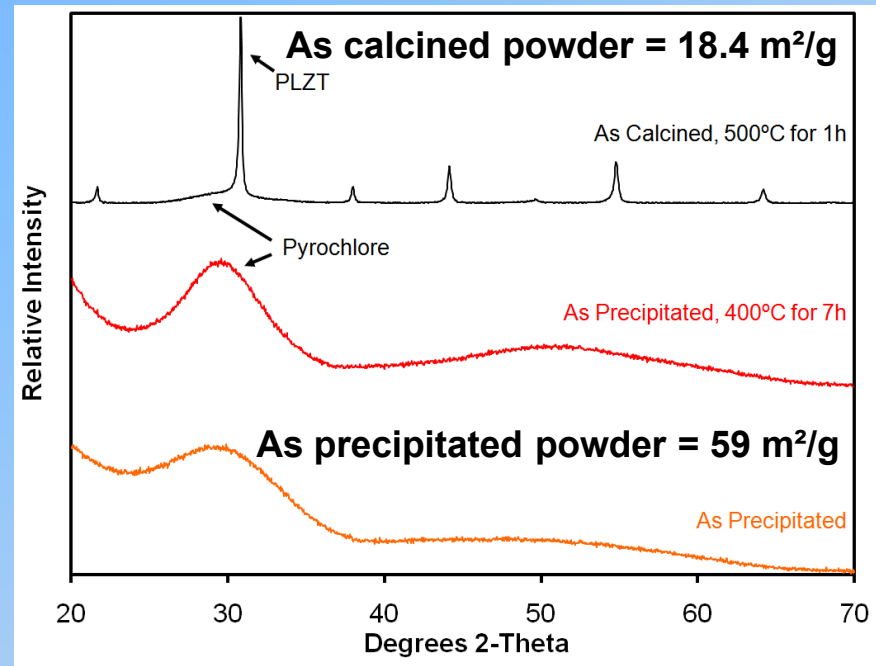
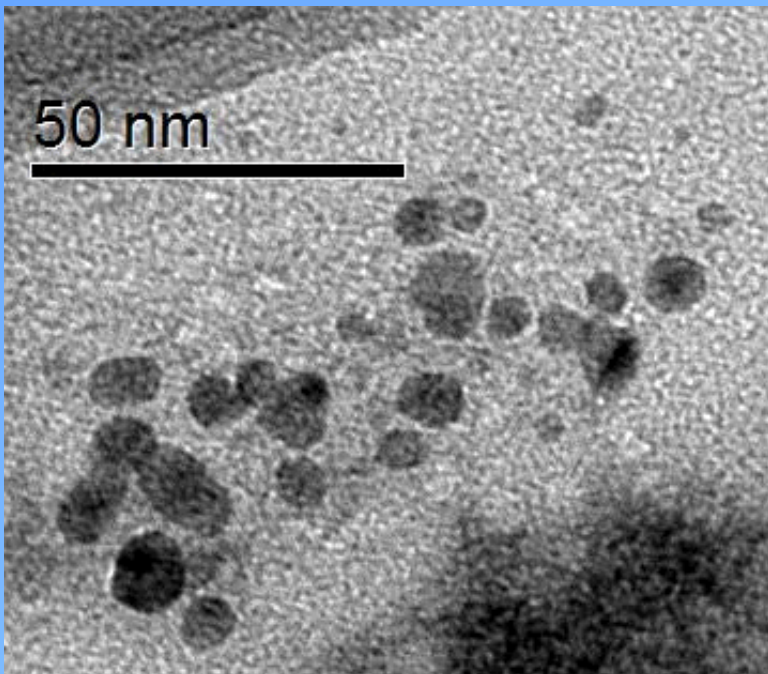
- $\text{Pb}(\text{NO}_3)_2$, $\text{ZrO}(\text{NO}_3)_2$ & La_2O_3 dissolved in HNO_3
- Diluted $\text{Ti}(\text{OPr})_4$



- Ammonium hydroxide to rapidly raise the pH
- Wash, centrifuge, and filter precipitate
- Dry amorphous precipitate with large surface area

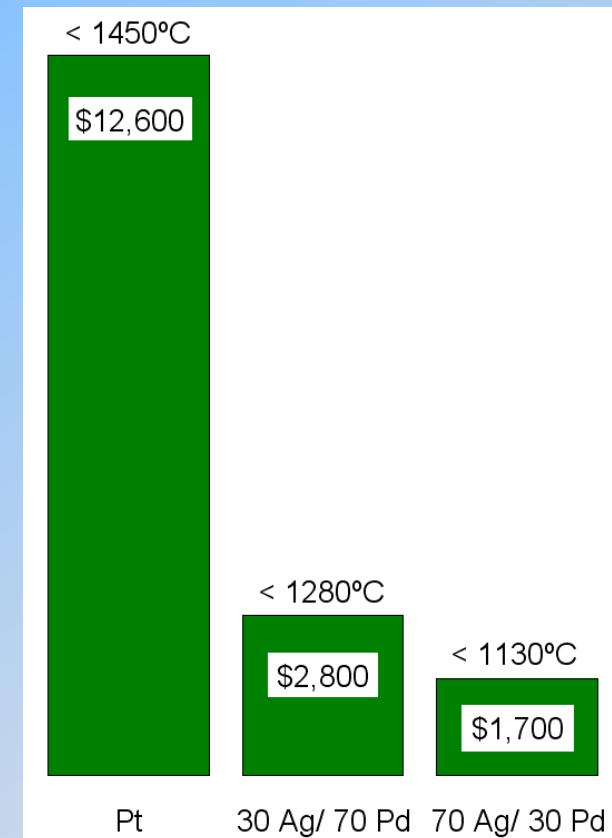
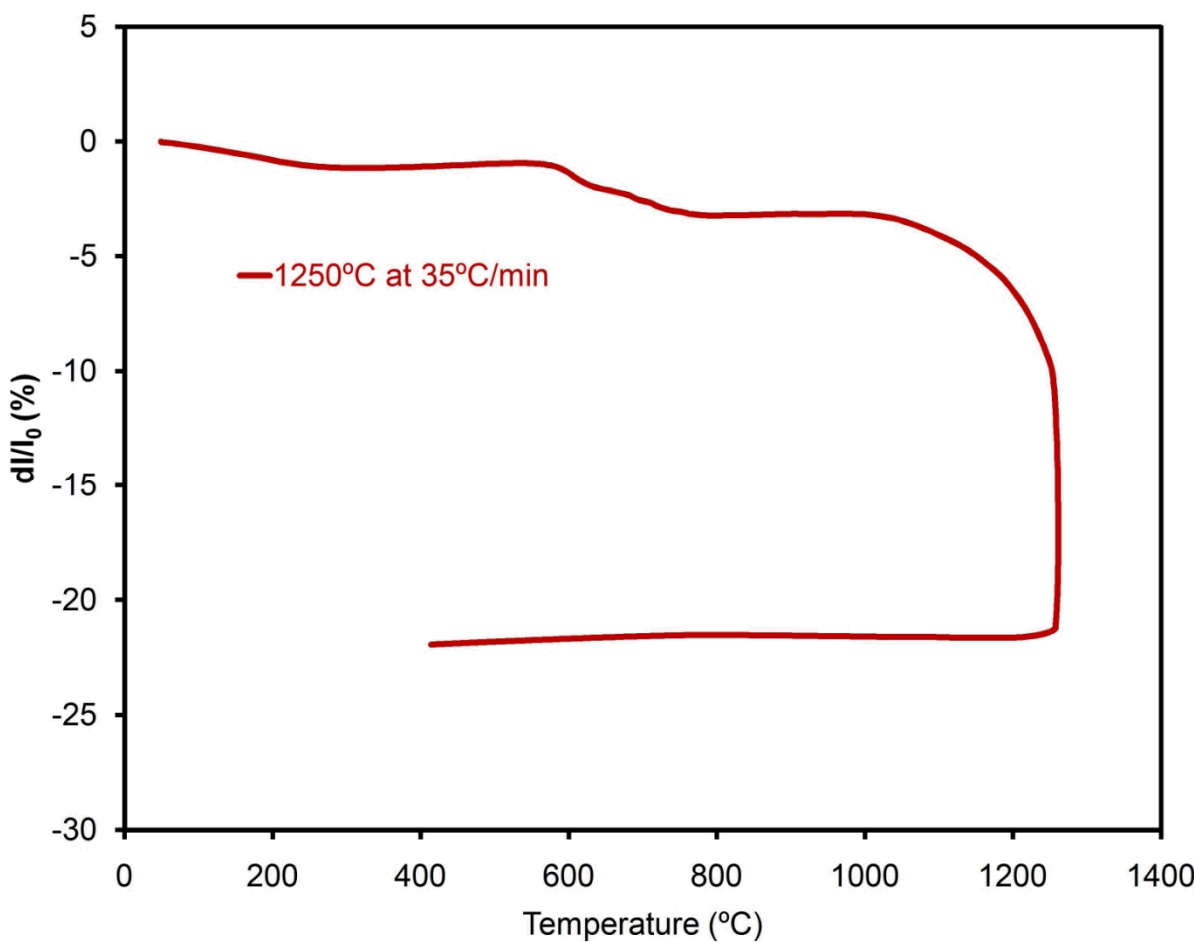


PLZT Nanoparticle Based Capacitors



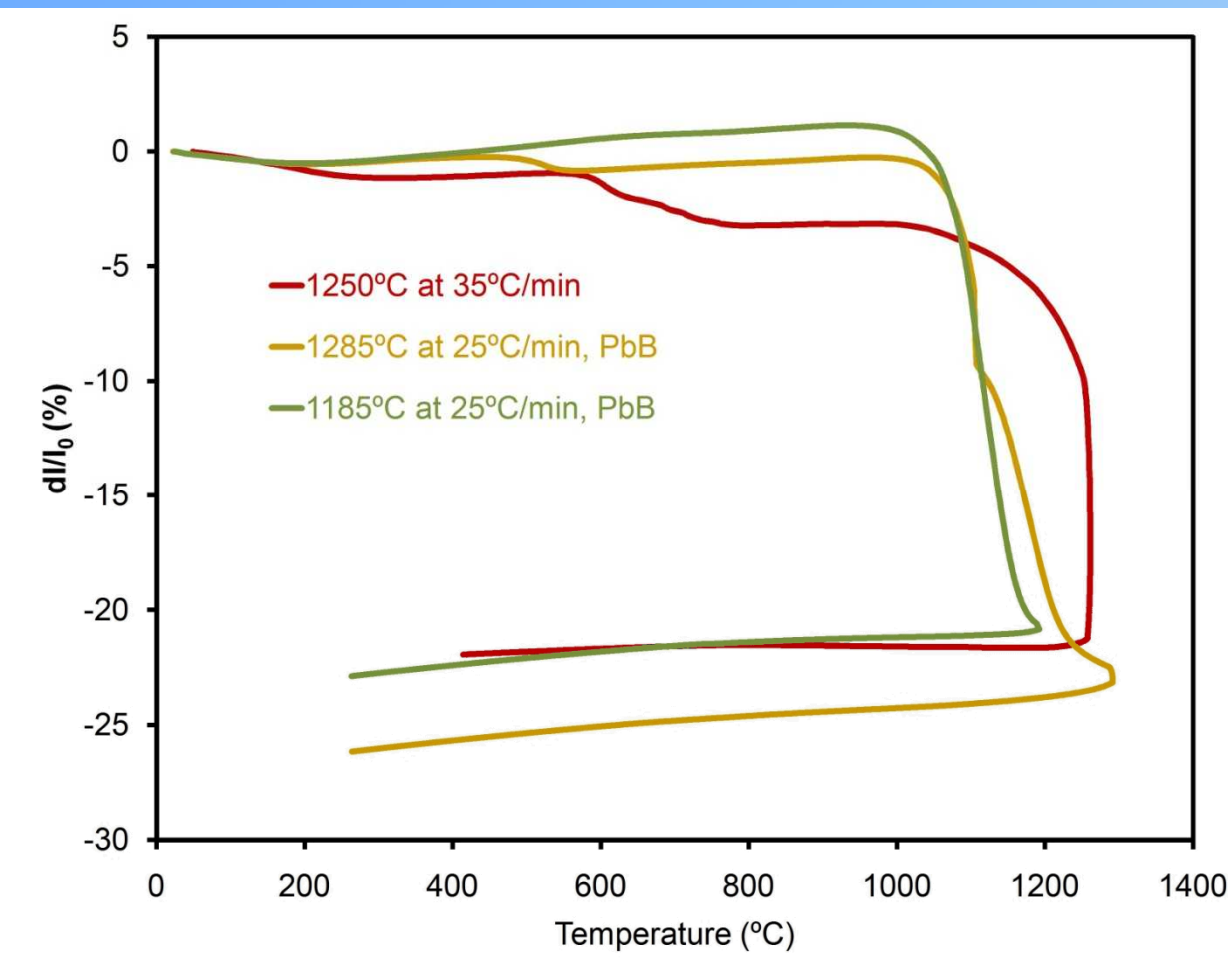
- Significant lowering of calcining temperature ($300 - 500^\circ\text{C}$)
- Crystallite size is reliably $< 100 \text{ nm}$ but the dry powder is agglomerated

Lowered Sintering Temperature



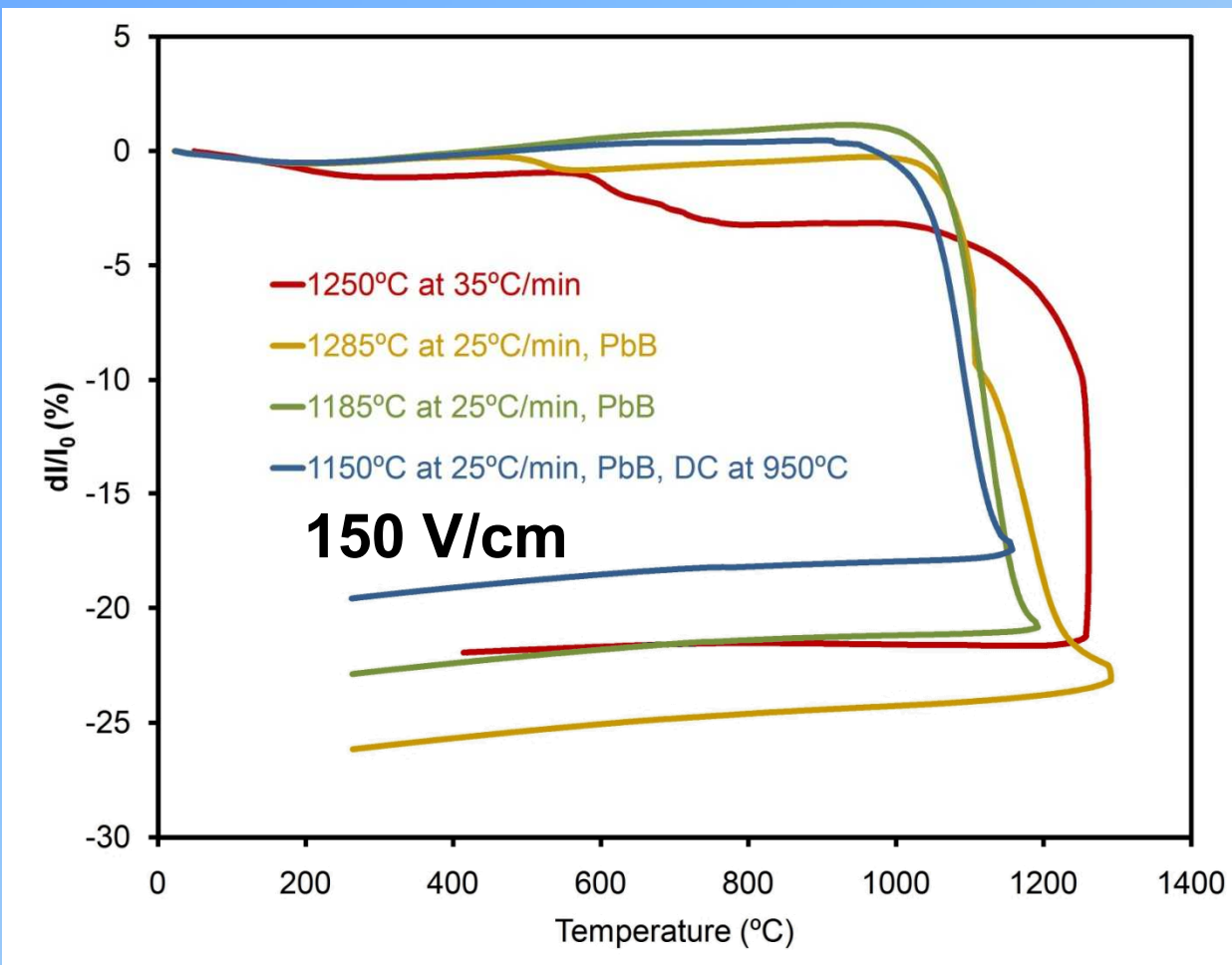
- > 4-fold decrease in electrode cost transitioning from Pt to 70/30 Ag/Pd
- Reduced lead volatility

Glass Sintering Aids



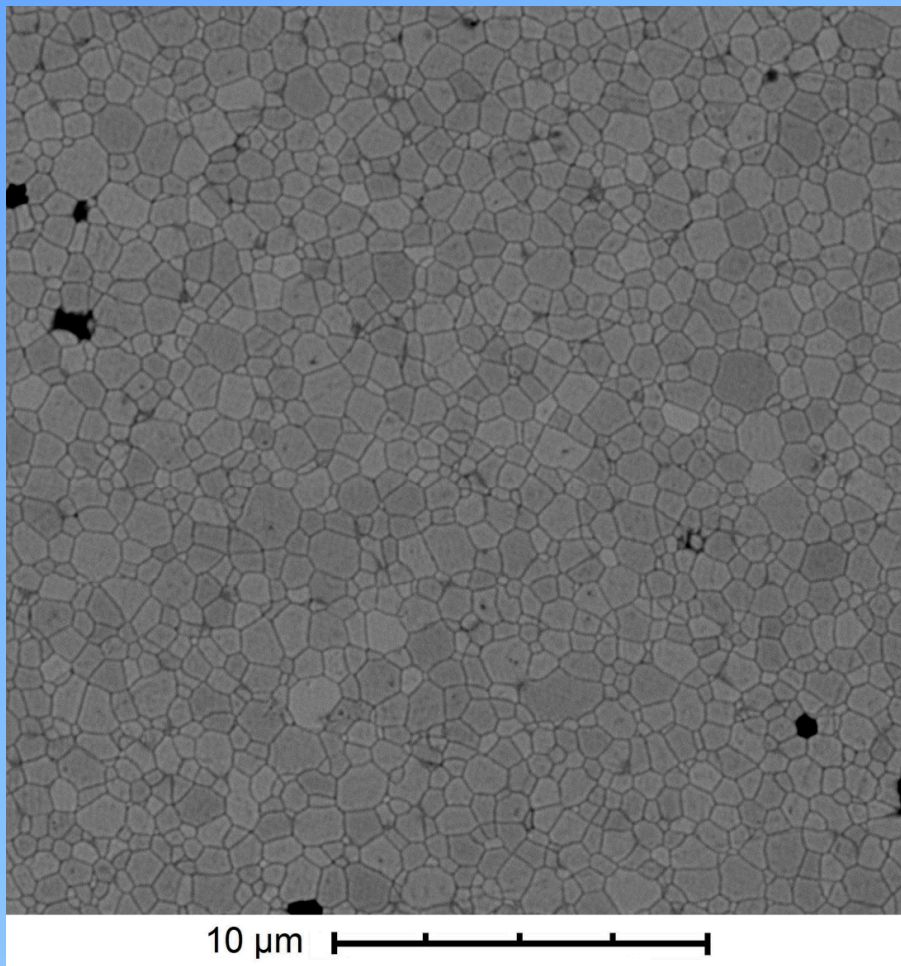
- 0.5 w/w loading
- Need to ensure glass does not detract from electrical properties

Electric Field Assisted Sintering



- Higher electric fields may result in even lower sintering
- Temperatures similar to spark plasma sintering

SEM of Sintered PLZT

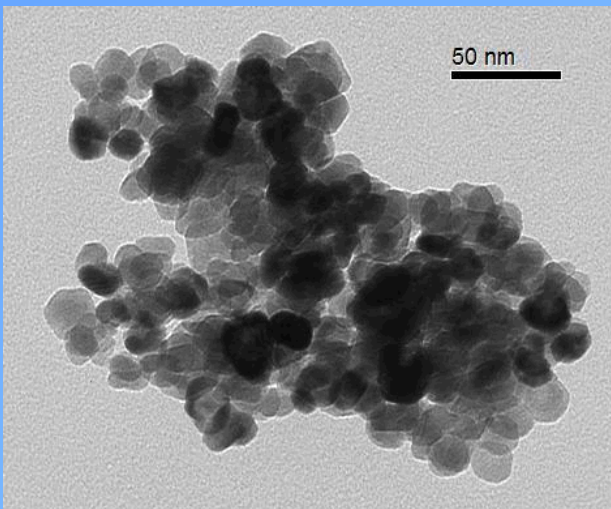


- Sintered with glass aid
- No field assist
- Good densification
- Some grain growth
- Possible grain pull-out during polishing

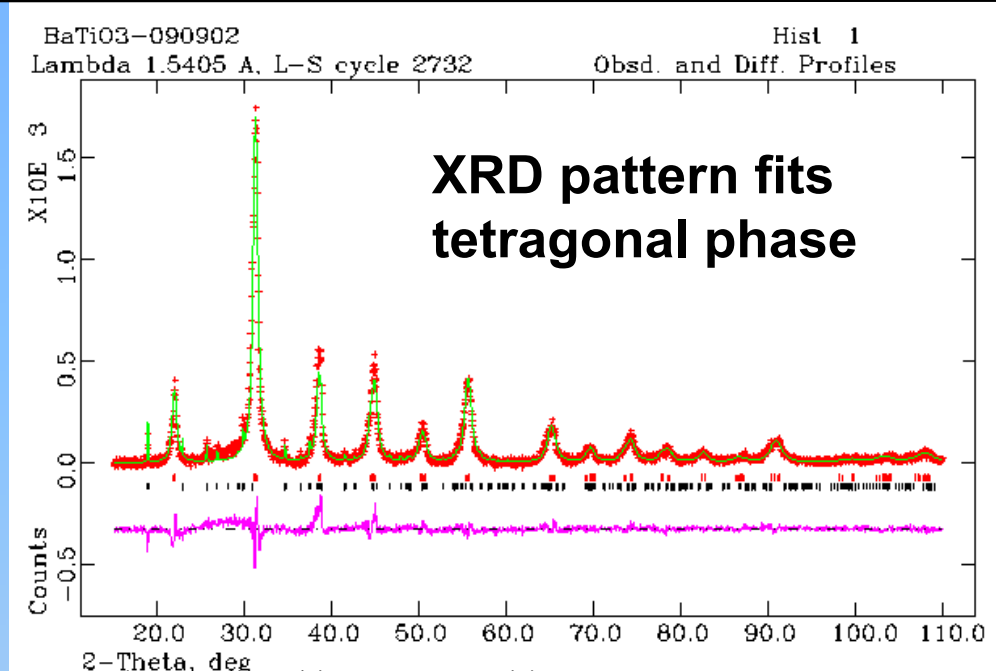
- All grains are $< 2\mu\text{m}$ with many sub-micron grains
- Electric field may assist densification with smaller grain

BTO

BaTiO_3 Nanoparticle Synthesis, $\text{Ba(OH)}_2 \cdot 8\text{H}_2\text{O}$ Reagent

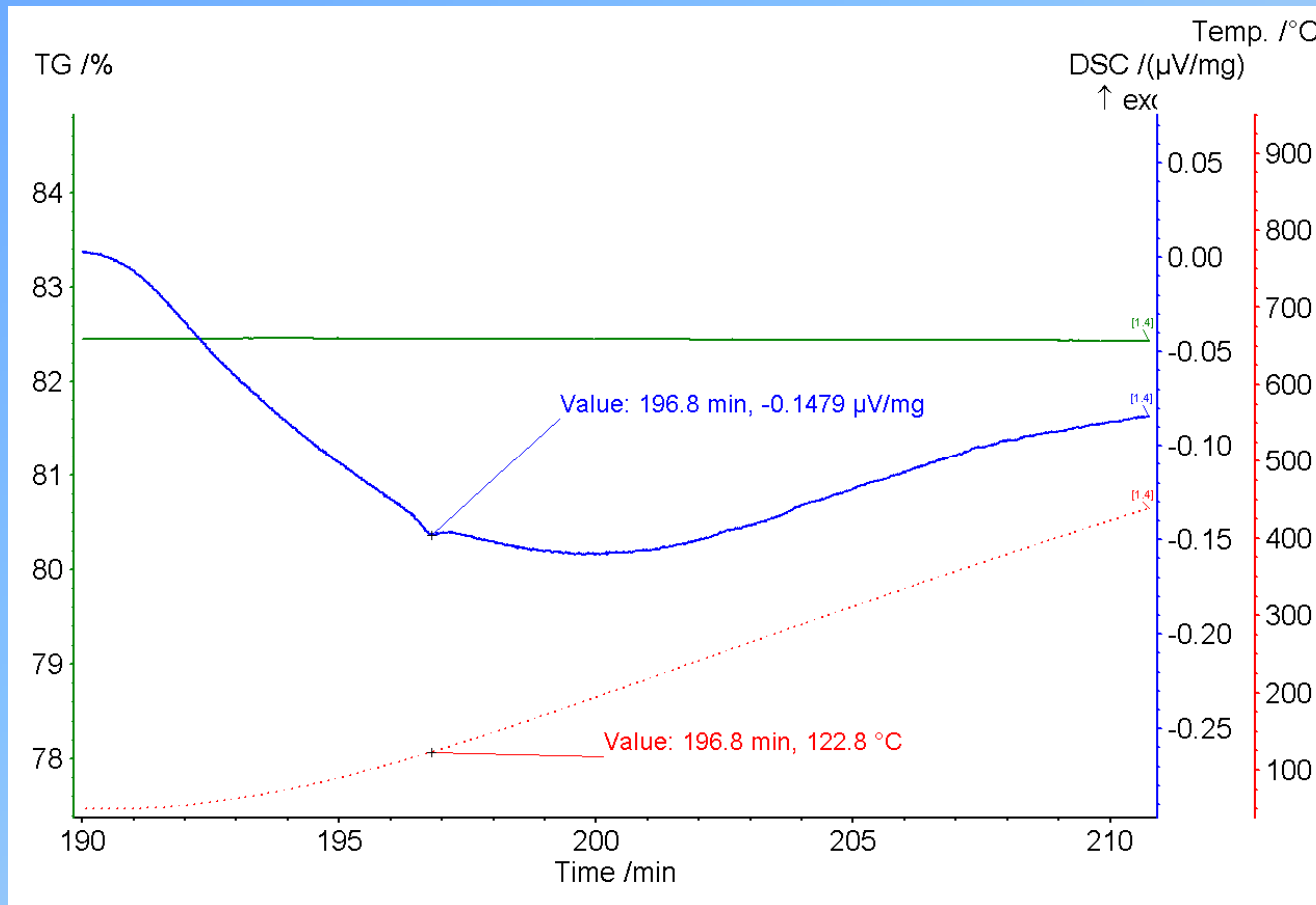


~ 10 nm diameter



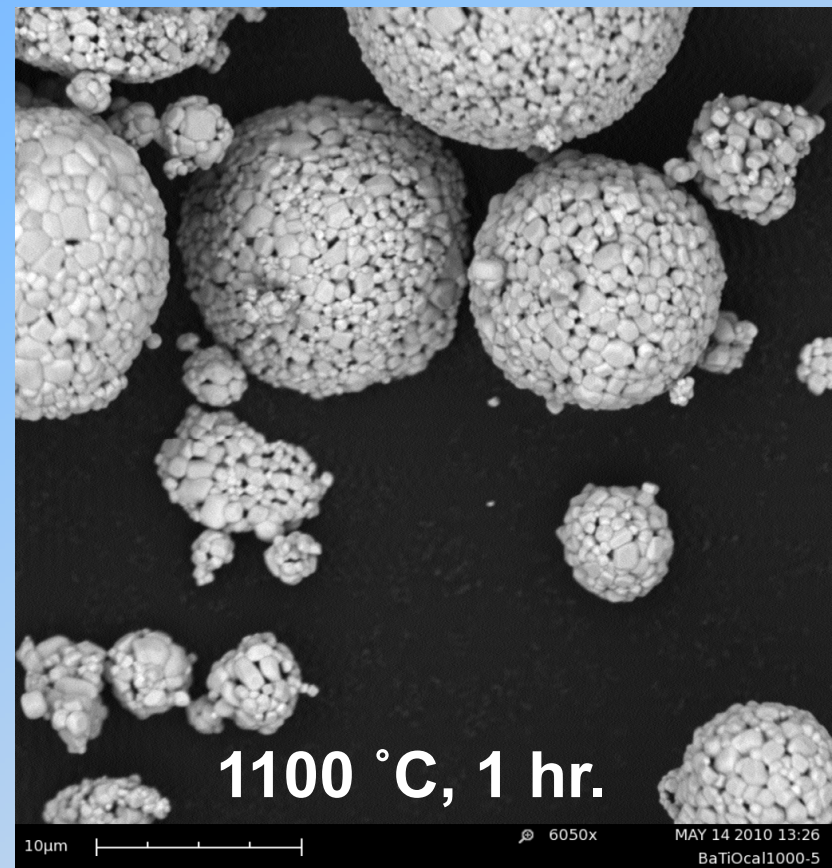
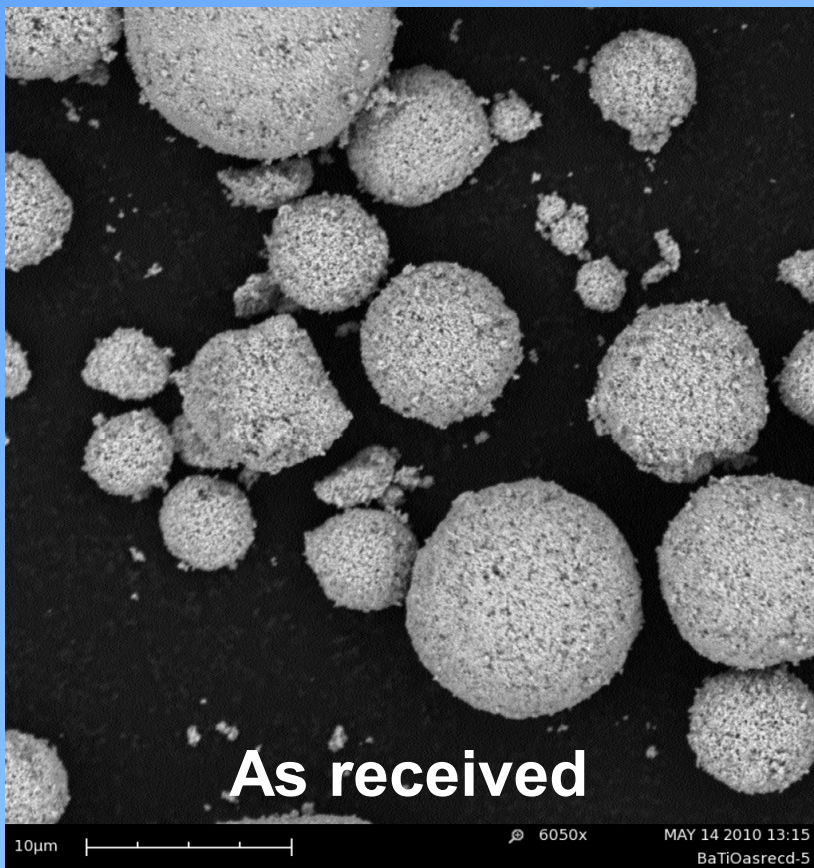
- $\text{Ba(OH)}_2 \cdot 8\text{H}_2\text{O}$ and Ti(OPr)_4 precursors at 80 °C
- Redesigned synthesis using air-free chemistry and with improved control over water addition
- Modified synthesis for our dry environment through extra H_2O addition
- XRD indicates tetragonal phase present when particles synthesized with 0.5 and 0.6 mol H_2O

BaTiO₃ Nanoparticle Synthesis, Ba(OH)₂·8H₂O Reagent



- Reheated BTO particles after initial cycle to 1300 °C
- Endotherm at 122.8 °C consistent with BTO Curie temp. (tetragonal → cubic phase transition)

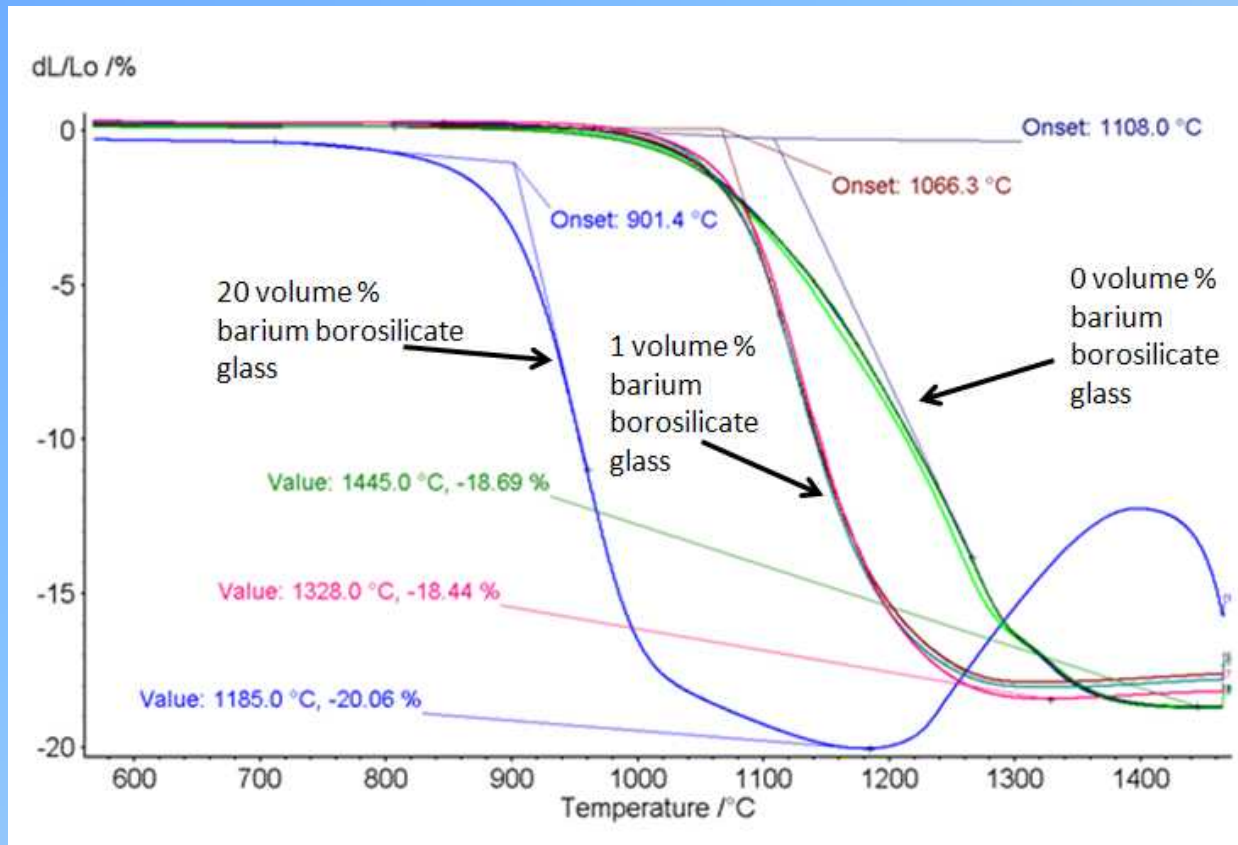
BaTiO₃ from TPL: SEM



- Primary particles of ~60 nm agglomerated into several micron clusters
- Coarsening of primary particles (~0.5 μm) with heating
- Breaking up agglomerates will improve homogeneity of composites

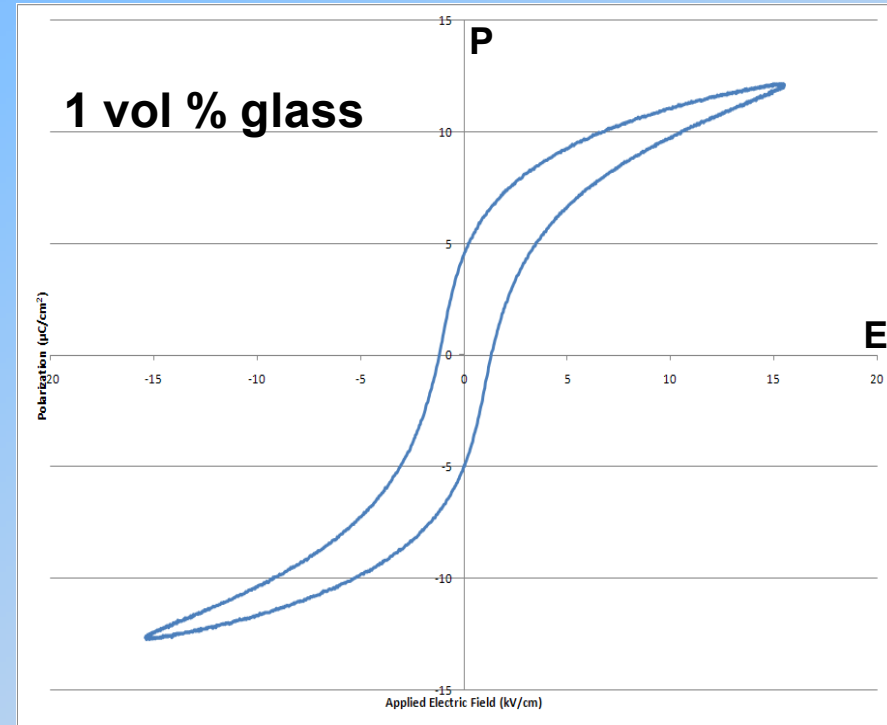
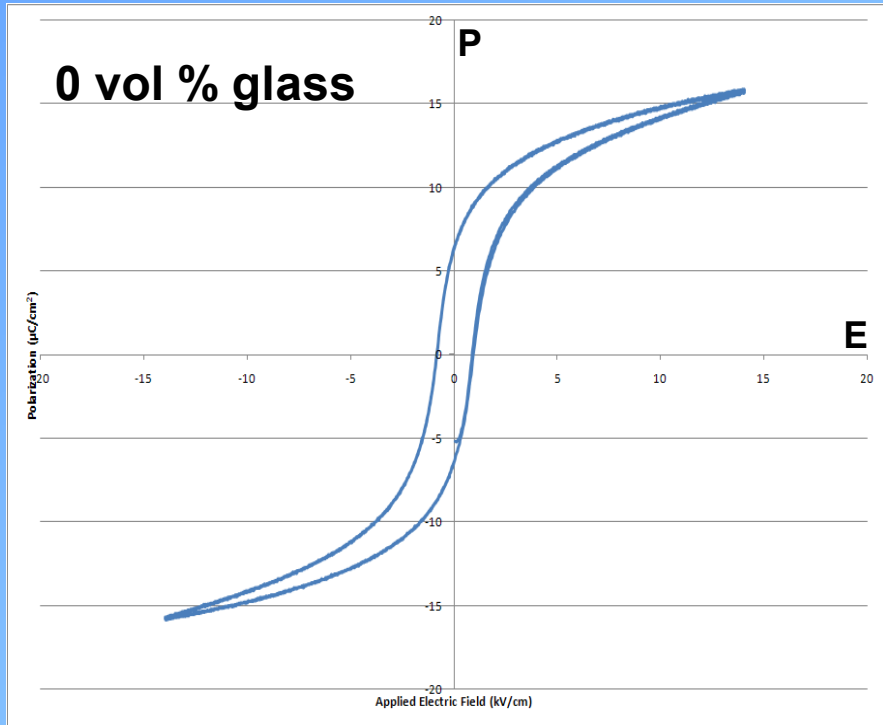
BaTiO₃ Nanocomposite Devices

Dilatometer sintering results



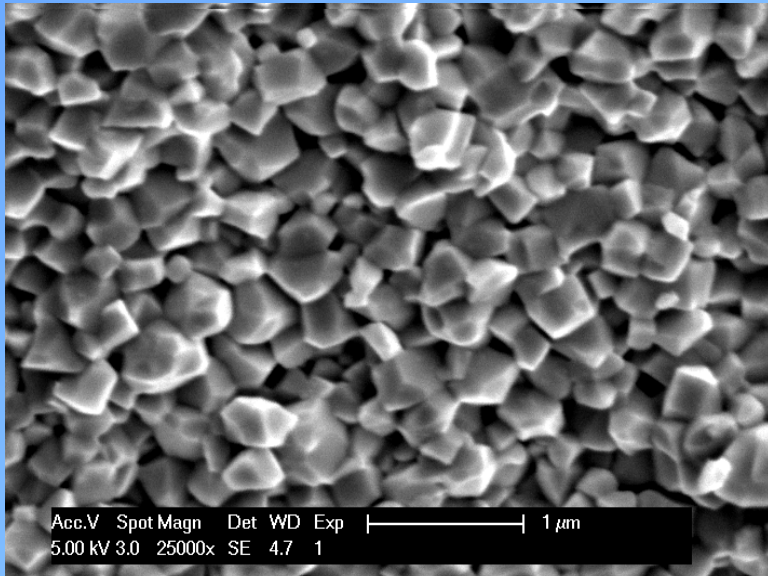
- Sintered TPL nano-BTO pellets from 0 - 20 vol% borosilicate glass loading
 - Sintering temp. reduced by almost 300°C through glass addition
 - Sample porosity also appears to decrease

BaTiO_3 Nanocomposite High Field Hysteresis

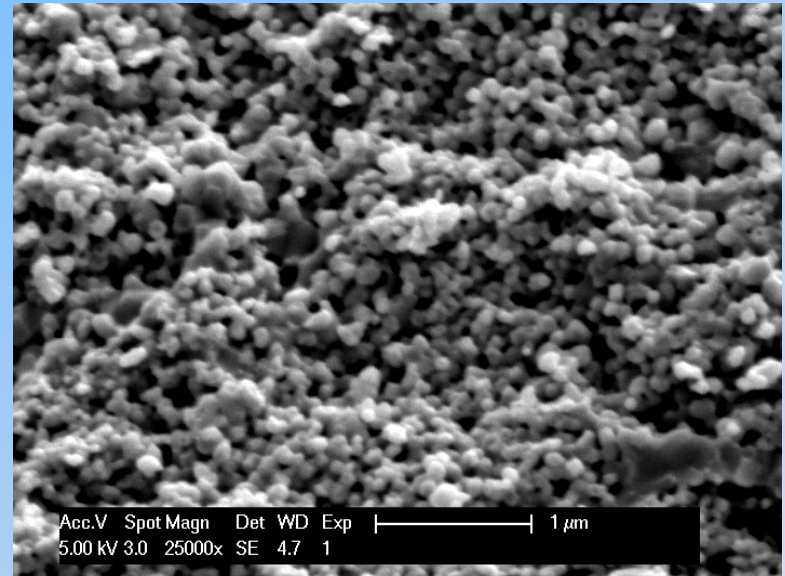


- More open hysteresis loop with the addition of glass

SEM of SPS BTO



TPL BTO, grain size 300 – 400 nm



SNL BTO, grain size 100 – 200 nm

- **Spark Plasma Sintering (SPS)**
- **BTO powders pre-calcined**
- **SPS at 950 °C**

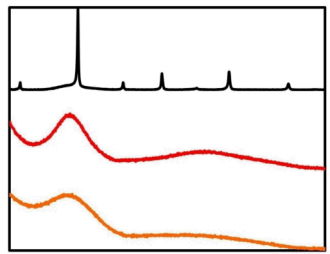
Conclusions - Ferroelectrics

- A scalable, environmentally benign synthesis route to generate nano-crystalline PLZT & BTO has been developed
- Several techniques to lower sintering temperature have proven effective and will assist fabrication of test devices
- Finding appropriate sintering aid amounts & chemistries + ideal sintering conditions (temperature, pressure, electric field, atmosphere) is crucial!

Acknowledgments

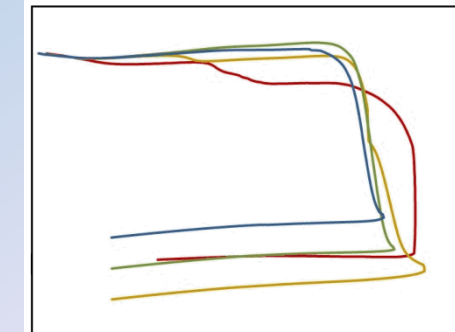
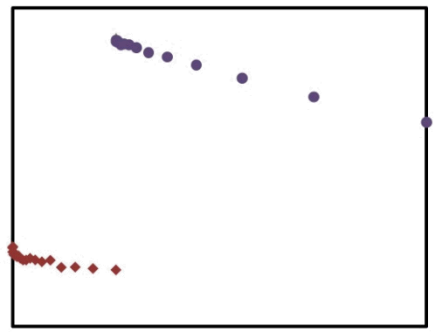
Mark Rodriguez

(XRD data collection & analysis)



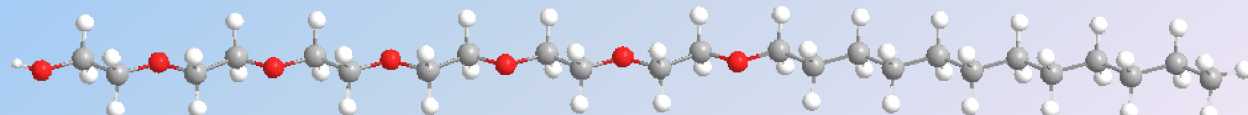
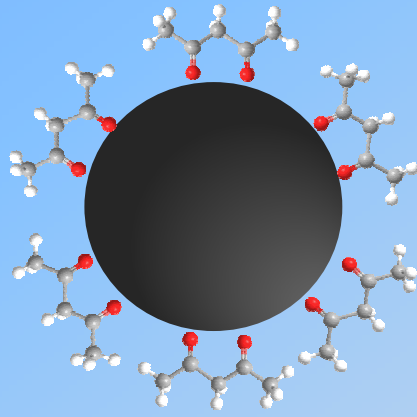
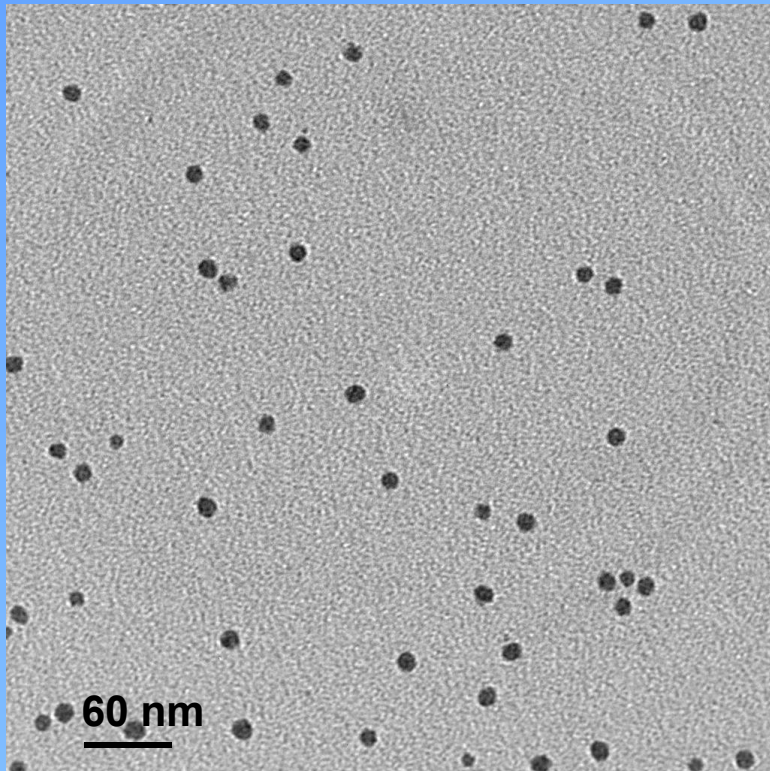
Future Work - Ferroelectrics

- Spray drying, thermal spray, and sonic dispersion (in combination with surfactants) will be examined to enhance particle dispersion
- Electric field assisted sintering and Spark Plasma Sintering (SPS) will be explored further
- More electrical results will be forthcoming
- All lessons learned processing PLZT will be applied to nano-BTO processing



Ferromagnetic Nanoparticles

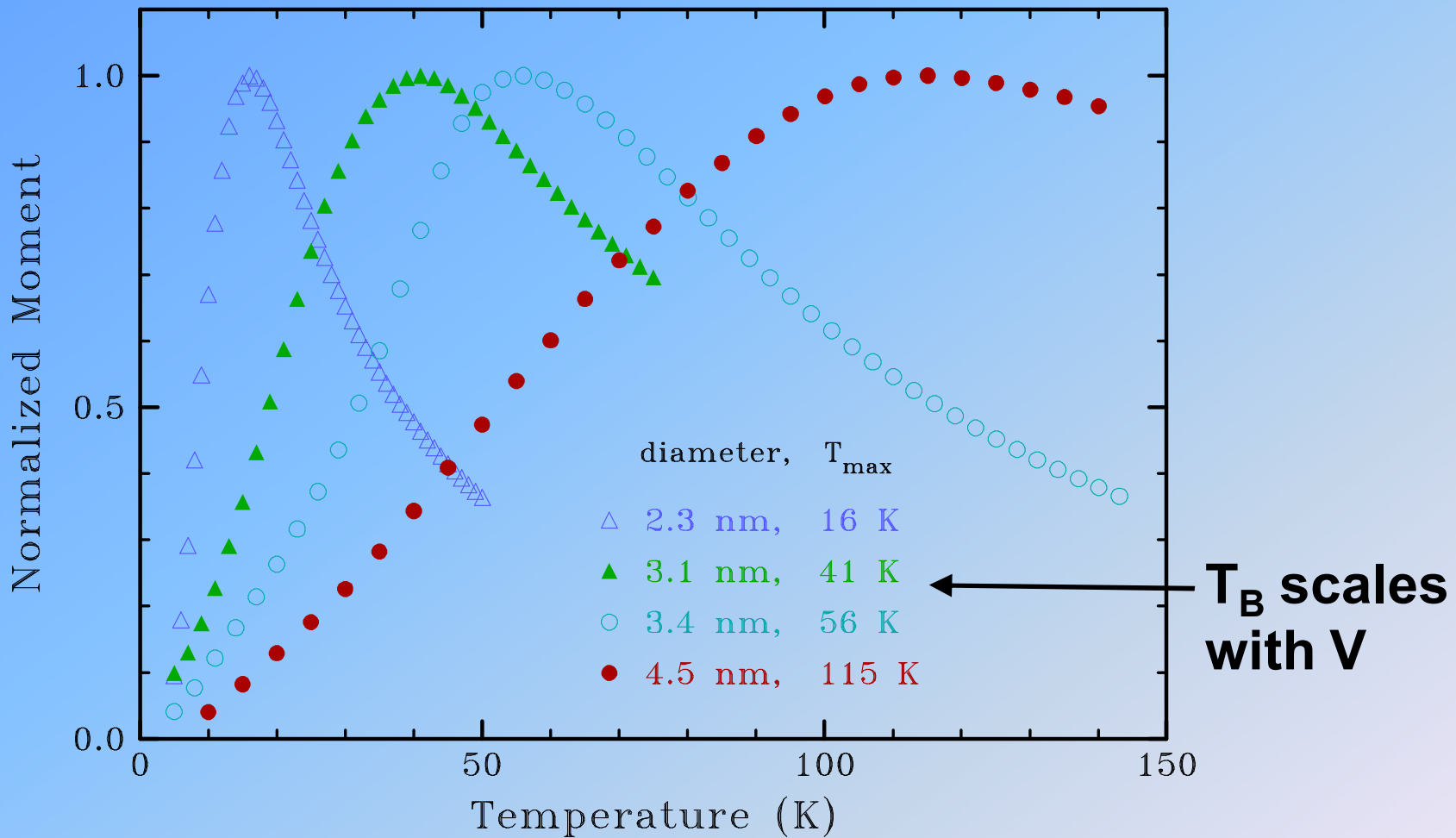
Fe Nanoparticles



- Thermal decomposition of iron pentacarbonyl in organic solvent
- Size control (2 – 10 nm diameter) through controlling ratio of iron pentacarbonyl to surfactant
- Synthesized with two surfactants: acetylacetone (2,4-pentanedione or PD) and hexaethylene glycol monododecylether (C12E6)
- Water and oxygen are carefully excluded through air free chemistry techniques

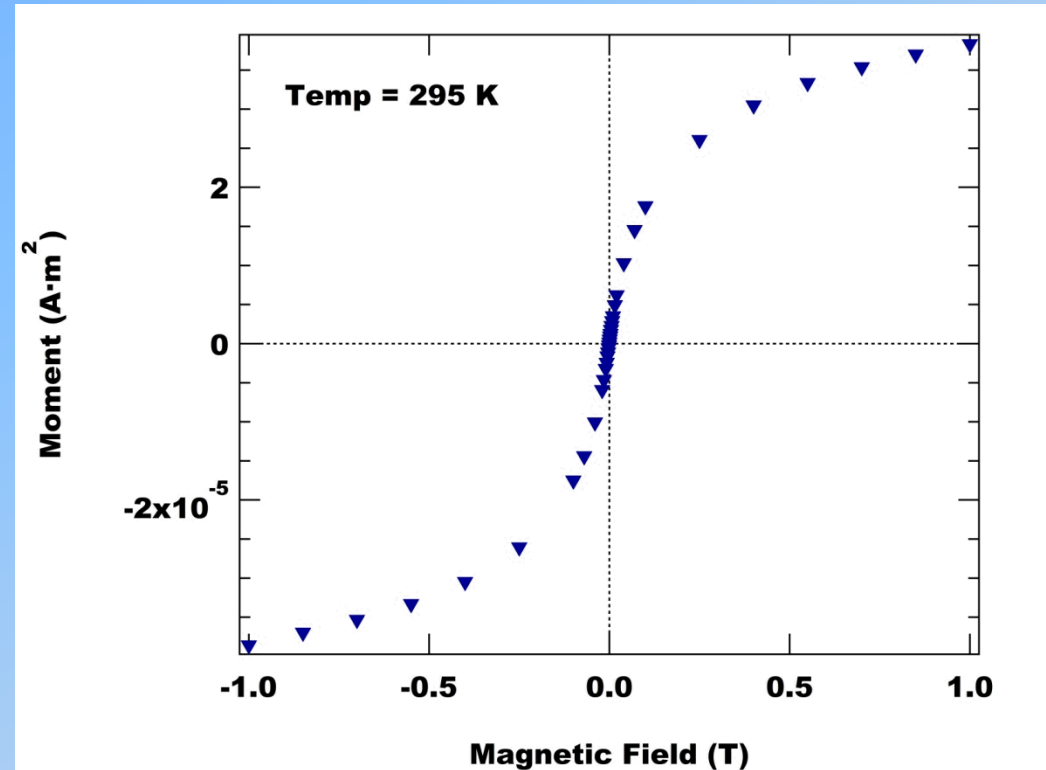
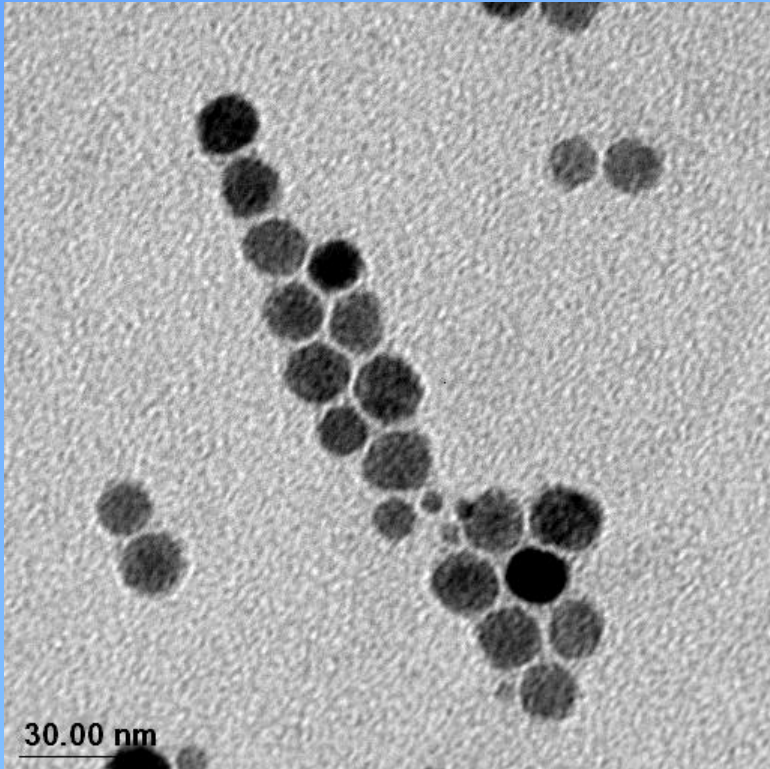
Huber et al, *J Magn Magn Mat* 278, 311 (2004)

T_B vs. Fe Nanoparticle Diameter



- All curves ZFC
- Broad peaks for larger particles expected
- Plotting σ vs. T/T_B peaks would superimpose

Fe₃O₄ Nanoparticles



- Fe₃O₄ Nanoparticles with poly(ethylene glycol) or PEG ligands
- Also possible to synthesize Zn_xFe_{3-x}O₄ and Ni_xFe_{3-x}O₄ nanoparticles (suitable for transformer core materials)

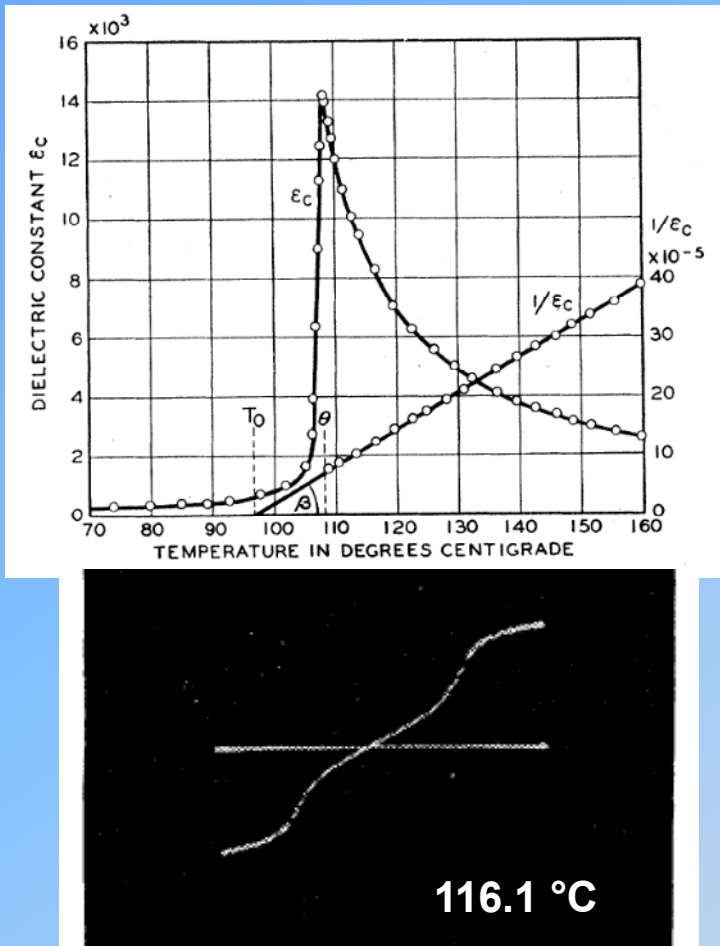
Extra Slides

Project Motivation & Goals

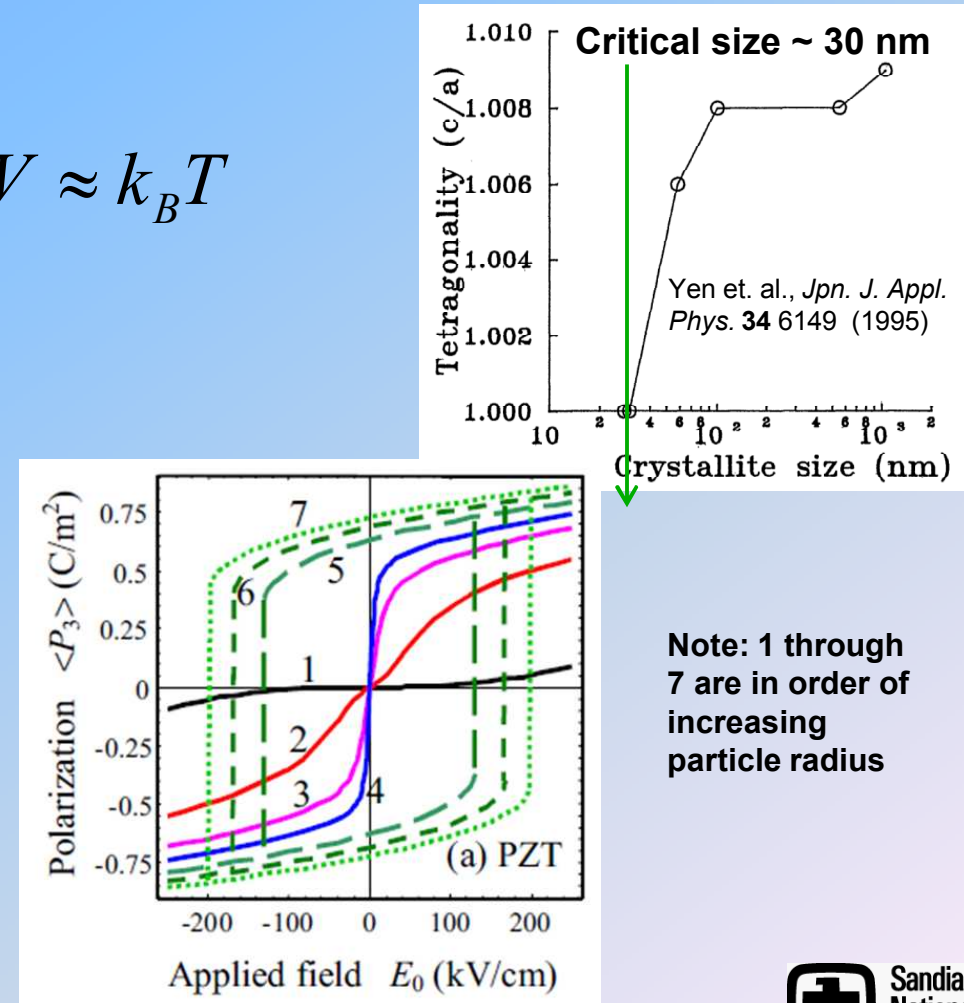
- Form composites with high volumetric loading of ceramic nanoparticles in a glass matrix
 - Achieve energy densities of 10 J/cc in robust devices with long shot life
 - Glass matrix will limit grain growth to preserve beneficial nanoscale properties of ferroelectrics
 - Glass will increase device breakdown strength (BDS)
- Develop BaTiO₃ & PLZT nanoparticle syntheses that will maximize device performance
 - Provide precise control over particle size and phase → allowing exploitation of size effects in ferroics
 - Tailorability of ceramic surface functionality to minimize grain growth and agglomeration while maximizing dispersion

Exploiting Size Effects for High Energy Density Dielectrics

Paraelectric \rightarrow Ferroelectric (cubic \rightarrow tetragonal) phase transformations can be induced in ferroelectric materials that have lost their spontaneous polarization



$$KV \approx k_B T$$

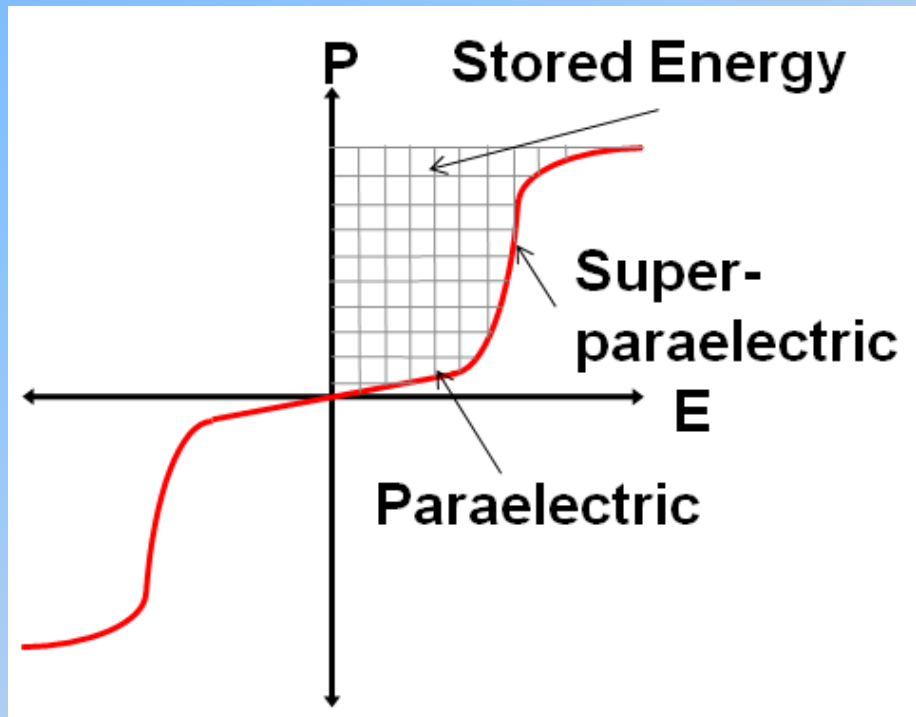


Merz, W. J., "Double hysteresis loop of BaTiO₃ at the Curie Point", *Phys Rev* 91 513 (1953)

M. D. Glinchuk, E. A. Eliseev, and A. N. Morozovska, "Superparaelectric phase in the ensemble of noninteracting ferroelectric nanoparticles", *Phys Rev B* 78, 134107 (2008)

Increased Energy Density Through Phase Transformation

- Increased energy storage possible through field induced phase transformation
- Transition BTO from cubic (paraelectric) to tetragonal (ferroelectric)
- Device hysteresis will allow energy densities $> 10 \text{ J/cc}$
- Nanoscale ferroelectric domains exhibit superparaelectric effect



BaTiO₃ Results

BaTiO_3 Nanoparticle Synthesis, Wada Synthesis Route

- > 100 nm BTO particles synthesized via thermal decomposition of barium titanyl oxalate in atmosphere or vacuum
- Synthesized BTO precursor, barium titanyl oxalate, via aqueous route using $\text{K}_2\text{TiO}(\text{C}_2\text{O}_4)_2$ and $\text{Ba}(\text{NO}_3)_2$

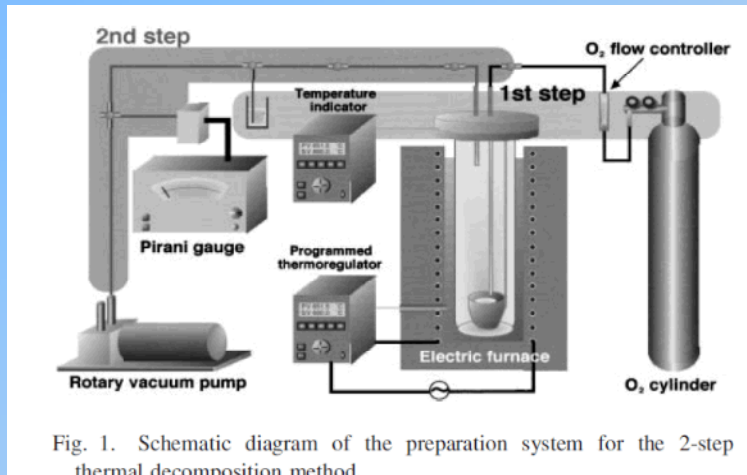
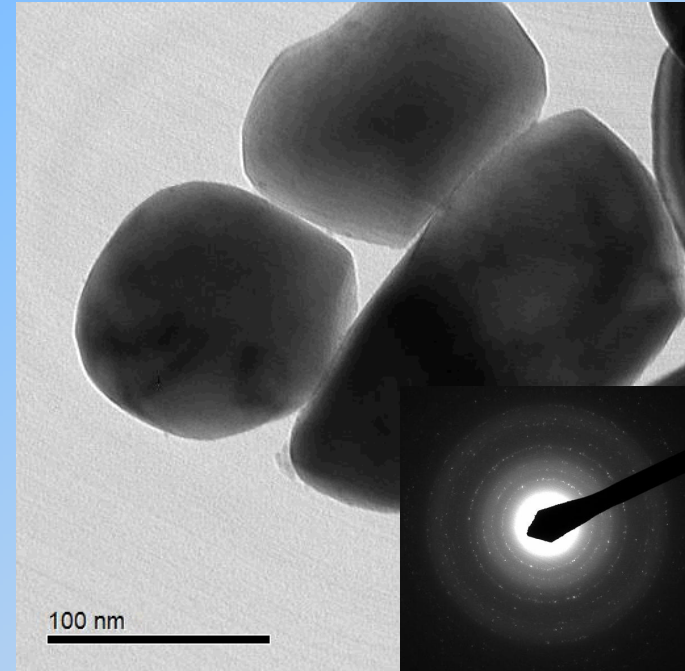


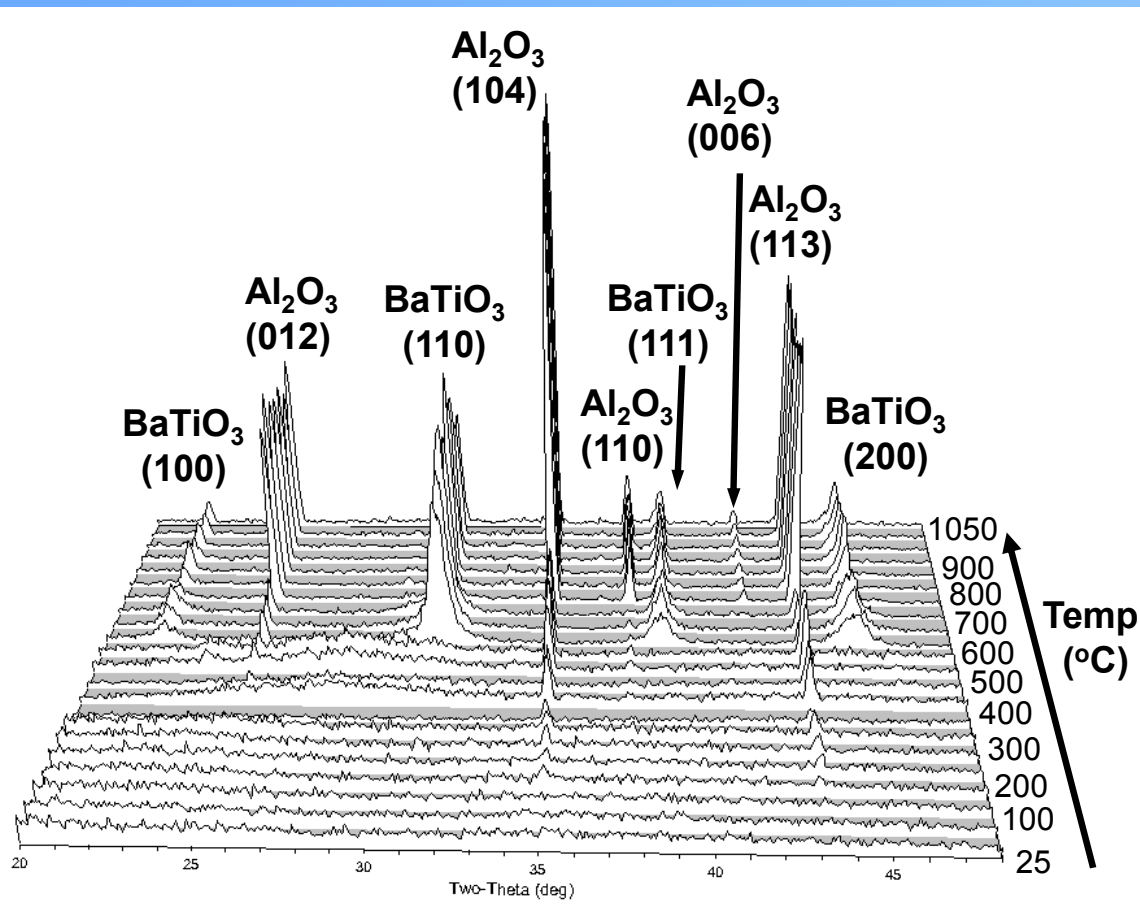
Fig. 1. Schematic diagram of the preparation system for the 2-step thermal decomposition method.



TEM image of BTO nanoparticles and SAED (inset)

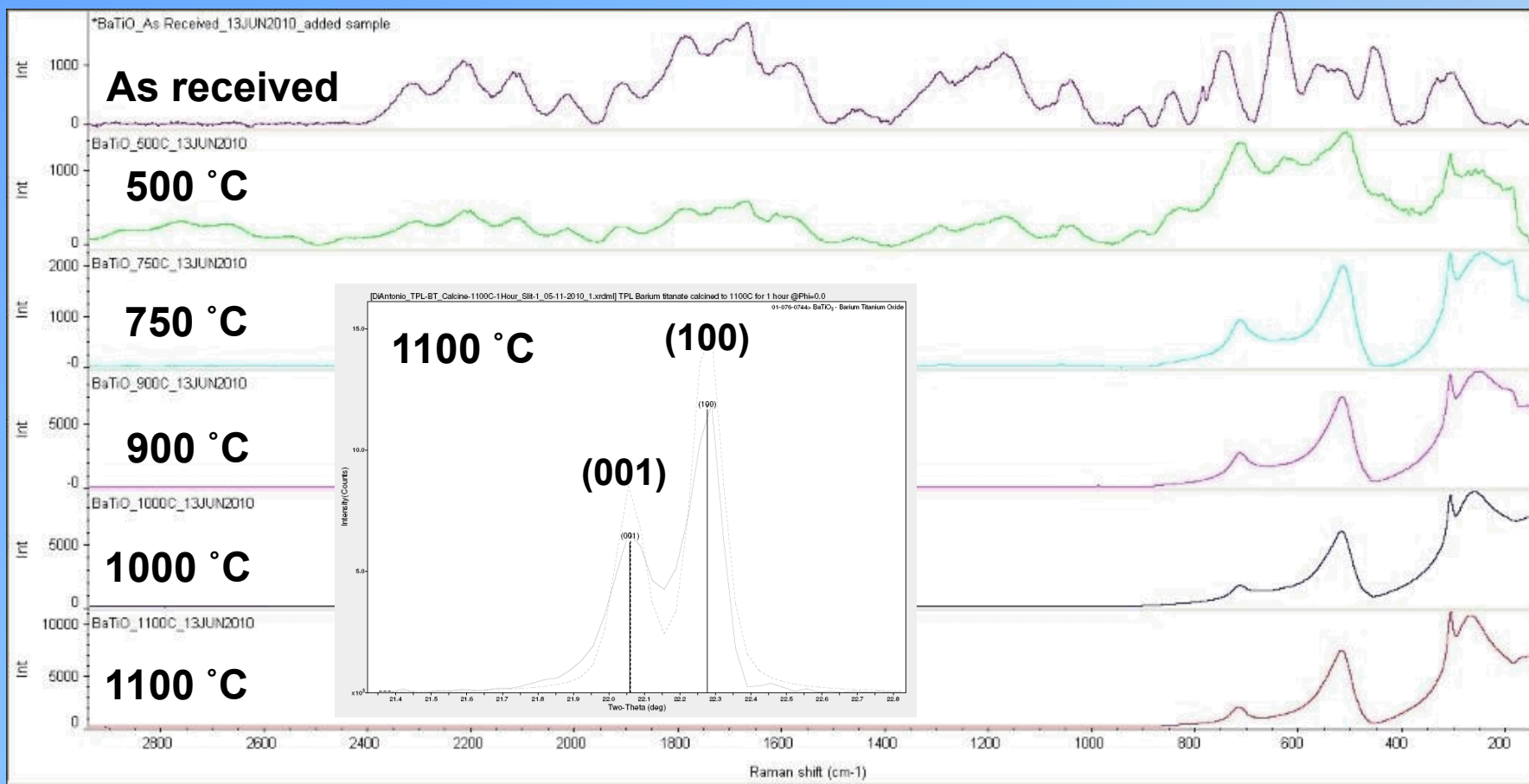
Hoshina et. al., "Size and temperature induced phase transition behaviors of barium titanate nanoparticles," *J. Appl. Phys.* **99** 054311 (2006)

High temperature XRD of Barium Titanyl Oxalate



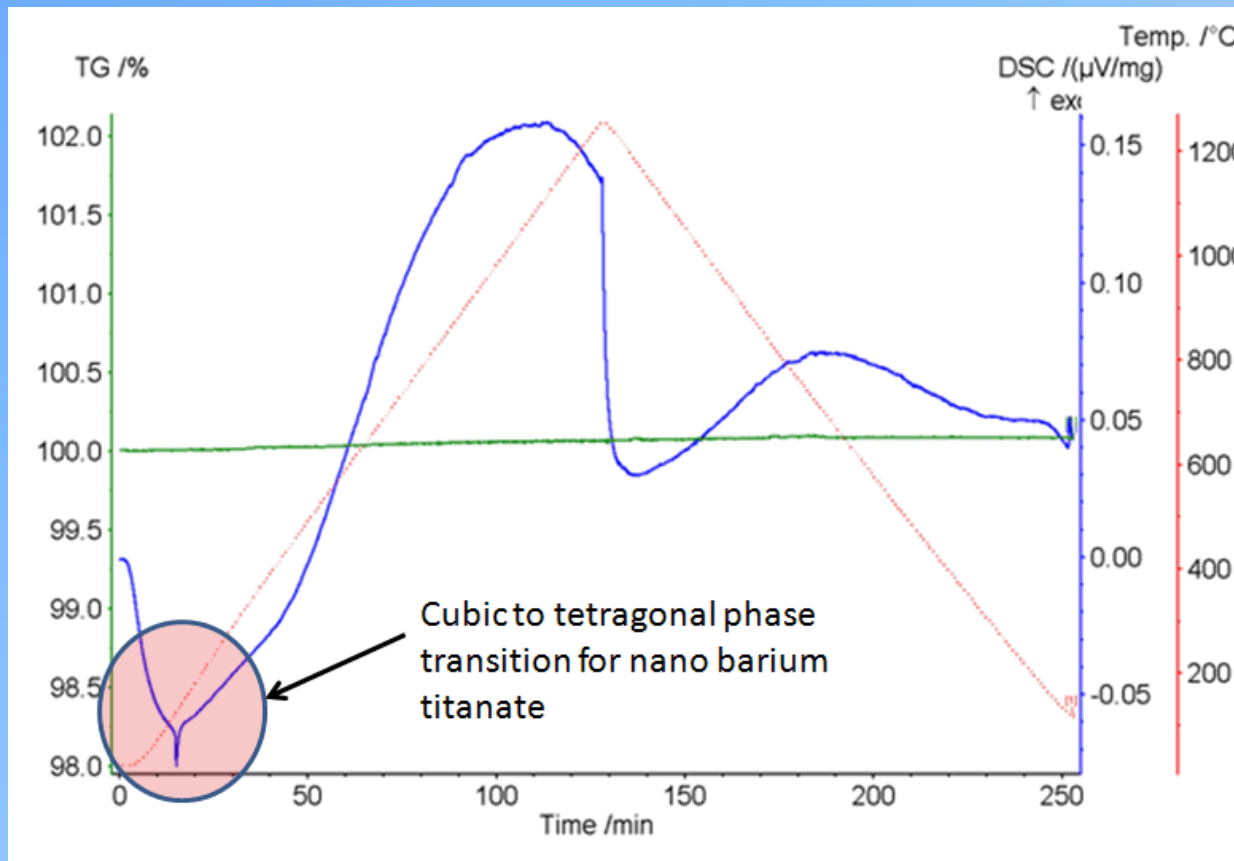
- Formation of strong amorphous pattern between 400 and 550 °C
- Crystallization of fine-grained BaTiO_3 at 600 °C, followed by further coarsening
- Al_2O_3 peaks appear at higher temperatures as the BTO powder consolidates and leaves the substrate area exposed

BaTiO₃ from TPL: Raman



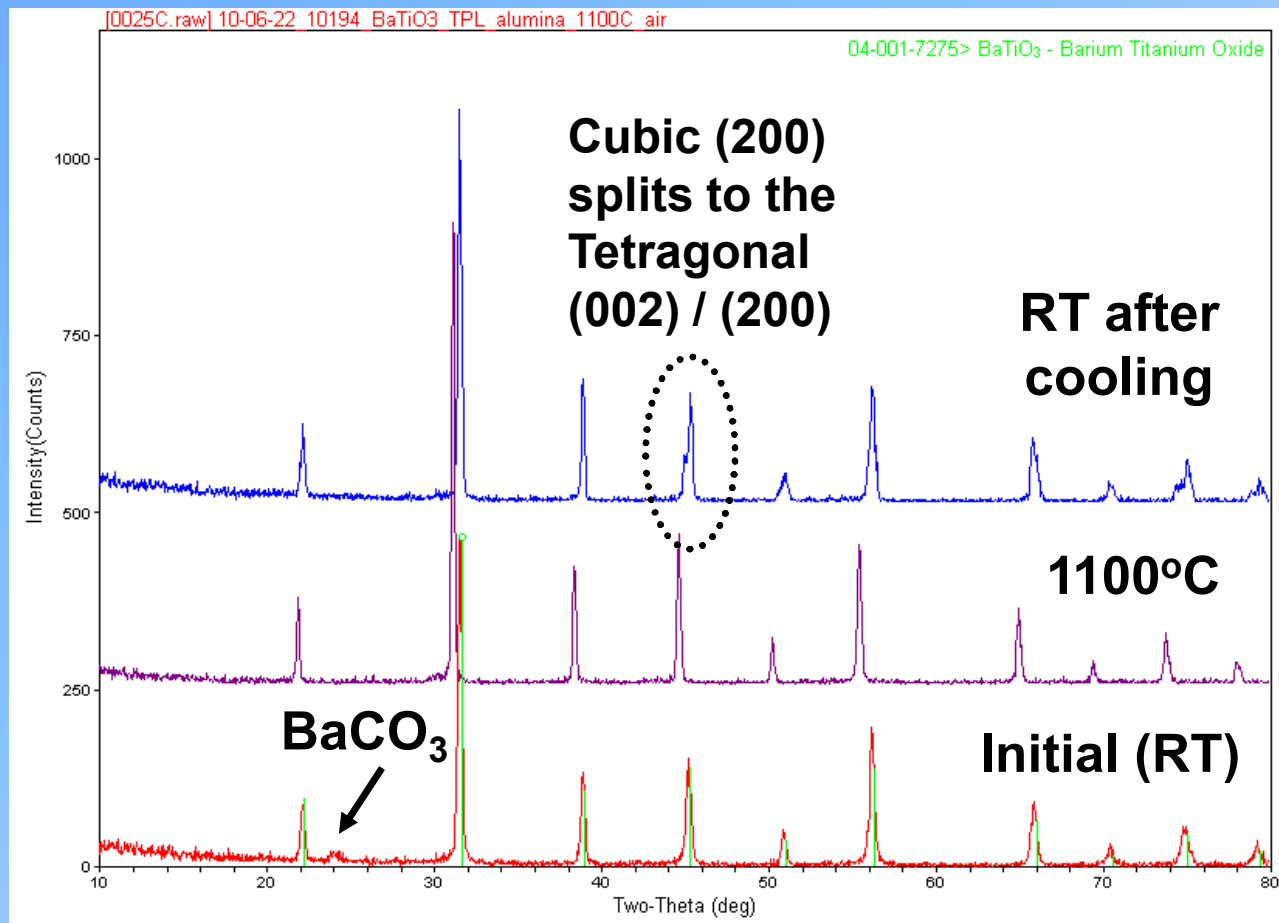
- Raman indicates conversion to tetragonal phase begins at 500 °C
 - Transition is complete at 800 °C
 - XRD shows splitting of (001) and (100) peaks after 1100 °C

BaTiO_3 from TPL: STA



- Simultaneous thermal analysis (STA)
- Tetragonal to cubic phase transition is apparent for calorimetric results (DSC or differential scanning calorimetry)
 - Phase transition only visible after heating to 1300 $^{\circ}\text{C}$

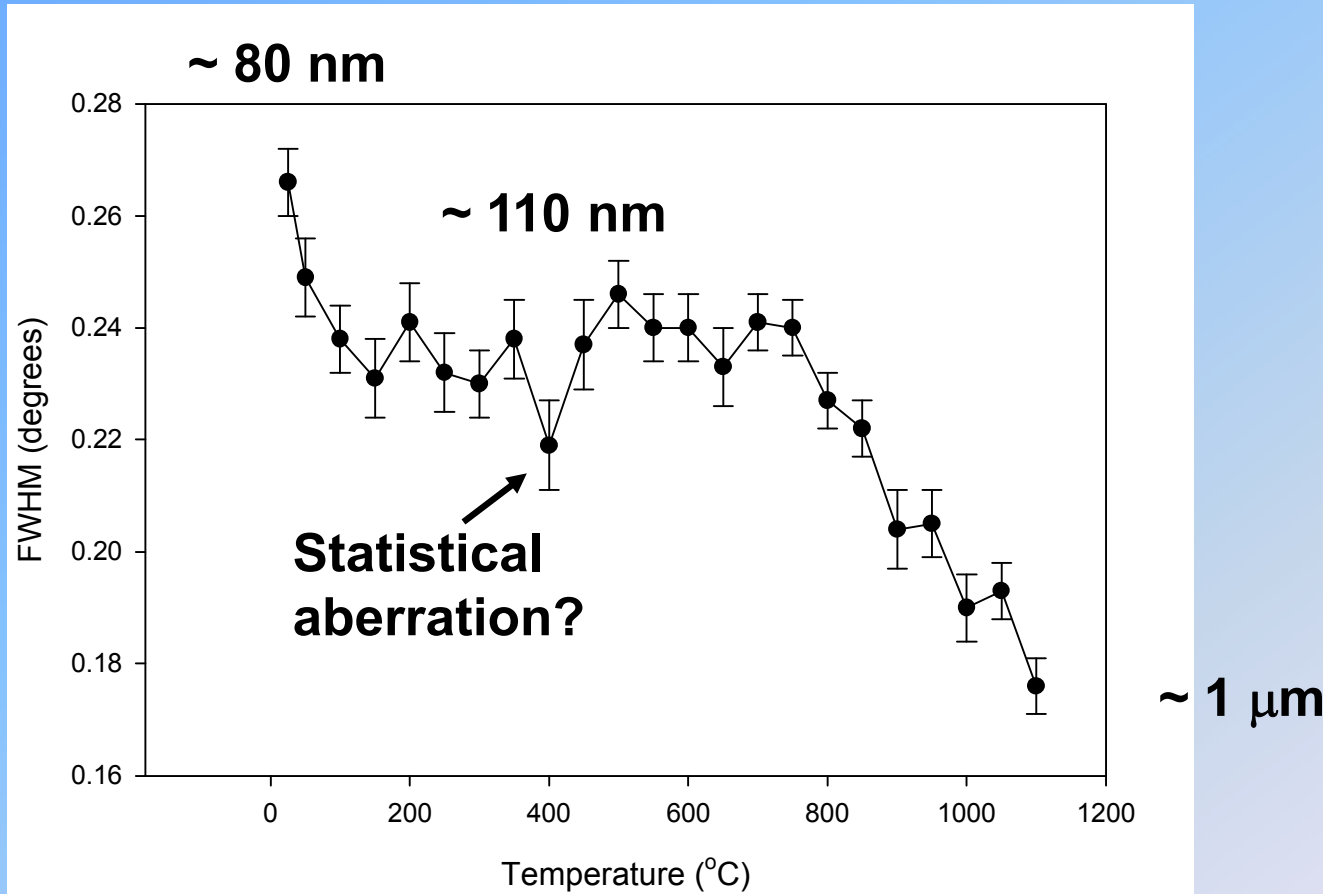
BaTiO₃ from TPL: High Temp. XRD



- TPL BTO shows an initial cubic structure
- peak sharpening of the cubic pattern at 1100 °C (grain growth)
- Tetragonal splitting of peaks upon cooling back to RT

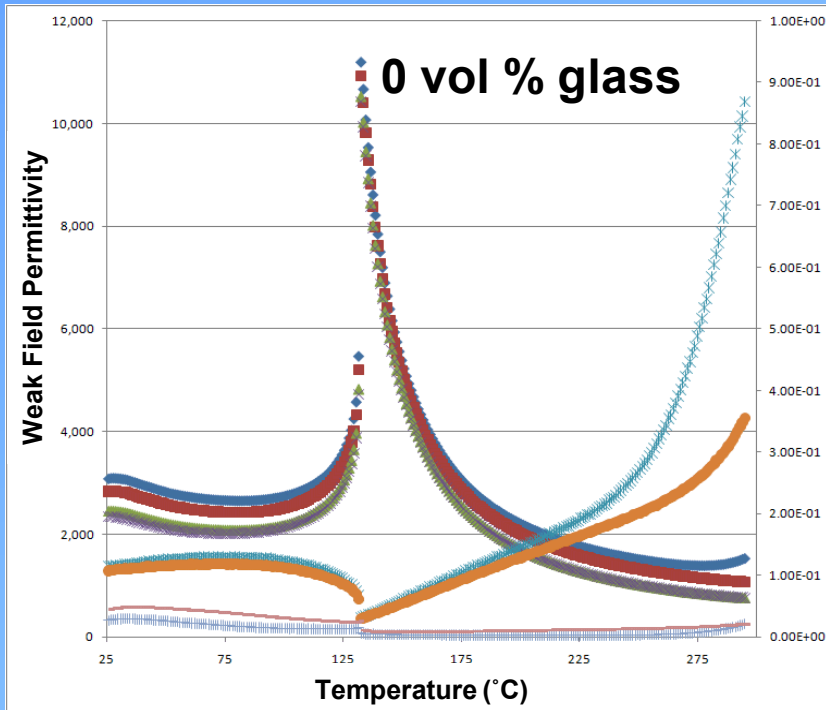
BaTiO_3 from TPL: High Temp XRD

BaTiO_3
(110)

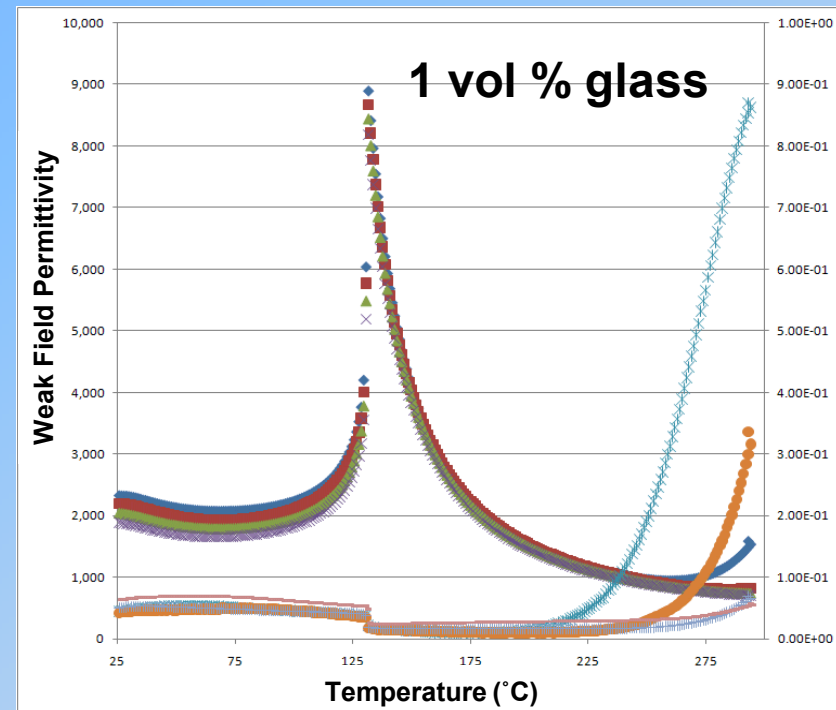


- FWHM for (110) BTO 100% peak shows decrease from RT to 150 $^{\circ}\text{C}$
- FWHM levels off until ~ 800 $^{\circ}\text{C}$
- Above ~ 800 $^{\circ}\text{C}$ we see another significant drop in FWHM

BaTiO₃ Nanocomposite Weak-Field Analysis



0 vol % glass



1 vol % glass

◆ 1kHz Permittivity
■ 10kHz Permittivity
▲ 100kHz Permittivity
× 1000kHz Permittivity

× 1kHz Loss
● 10kHz Loss
+ 100kHz Loss
- 1000kHz Loss

- Some change in dielectric loss with the addition of glass

Barium Borosilicate Glass

Components	Mole %	Weight %
BaO	50	68.73
SiO ₂	20.97	11.29
Al ₂ O ₃	102	0.93
H ₃ BO ₃	24	14.97
ZrO ₂	2.01	2.22
SrO	2	1.86

- Glass sintering aid for BTO/glass nanocomposite
- Provided by Missouri University of Science and Technology

BaTiO₃ Nanocomposite

High Field Hysteresis

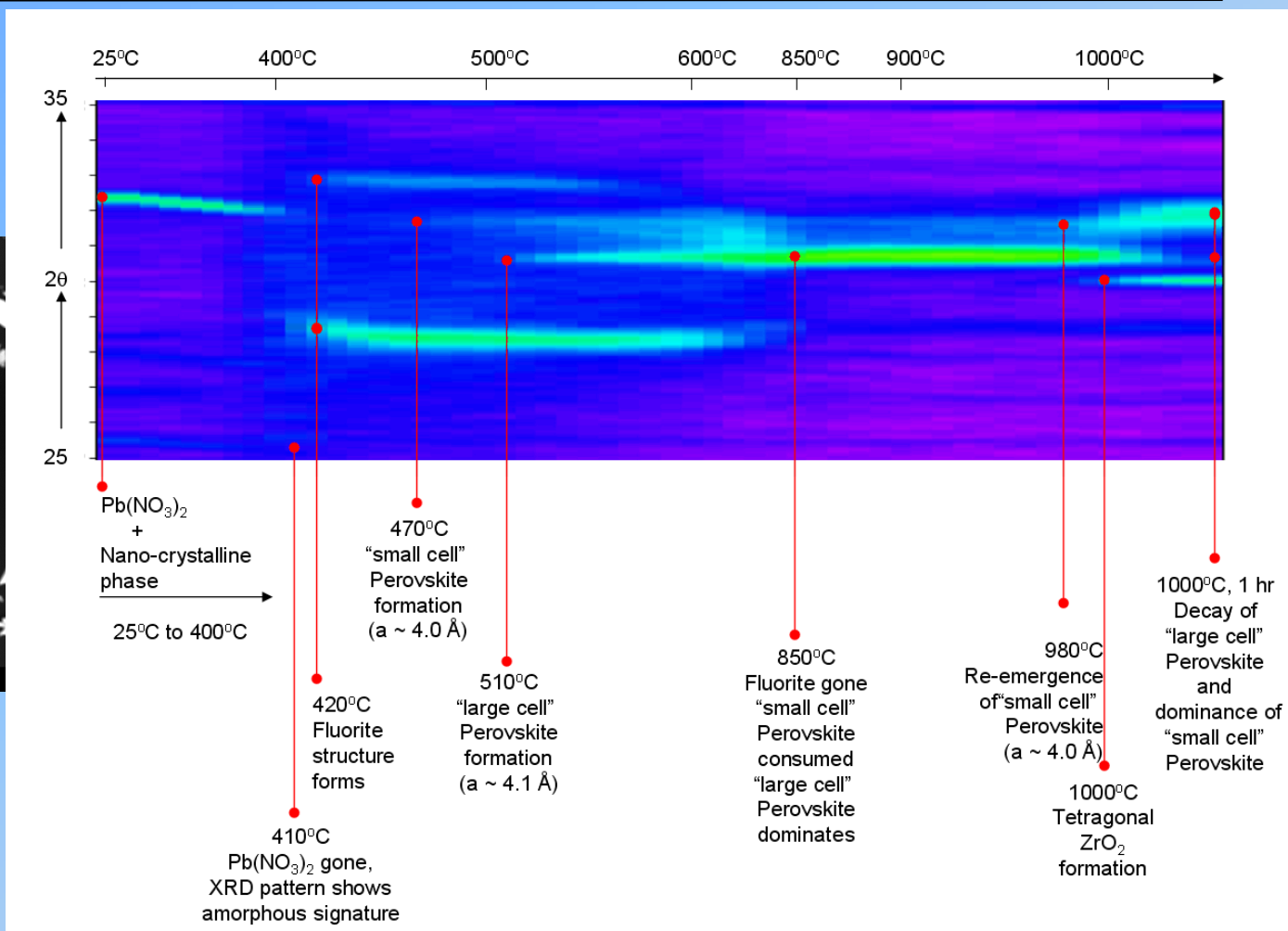
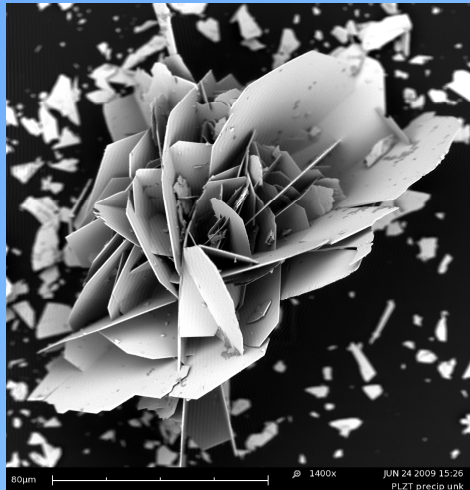


BTO/epoxy nanocomposite

- Epoxy composites will allow rapid testing of different BTO particle syntheses and sizes & optimize system
- Master Bond EP30HT and TPL BTO, 50 w/w %
- We will form composites with BTO nanoparticles that we synthesize next
- Cures with low porosity
- Beginning to dice and coat with electrodes for electrical testing

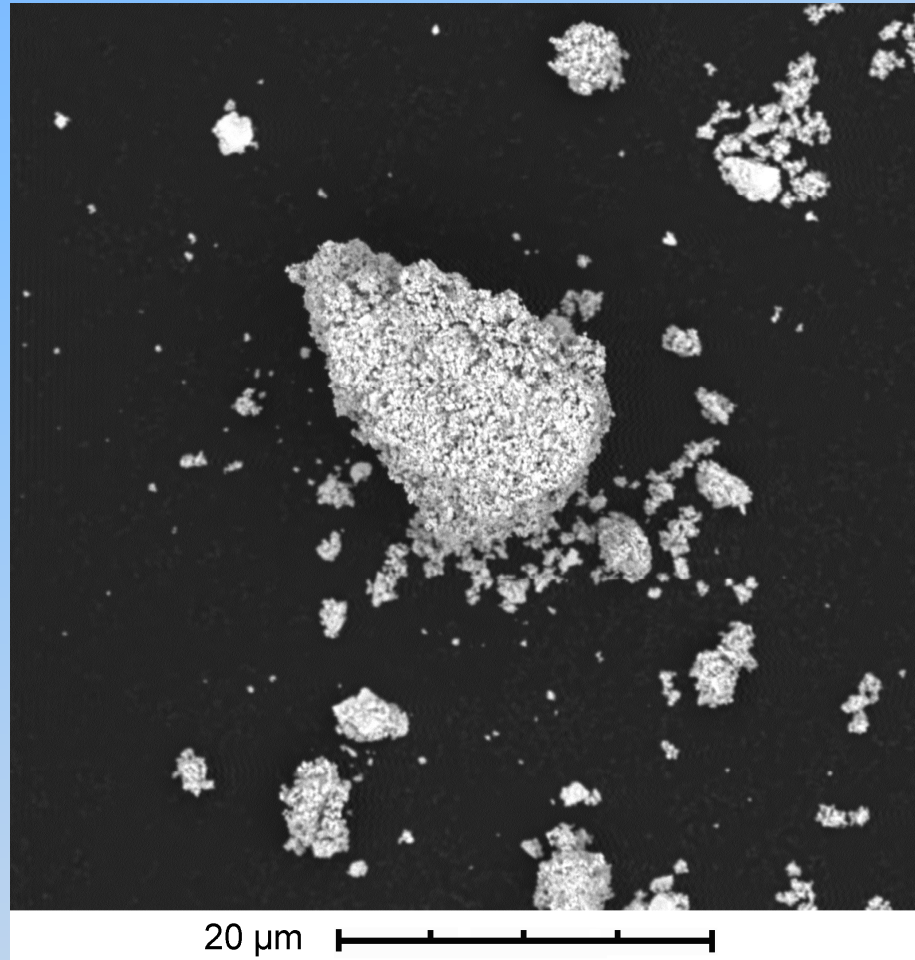
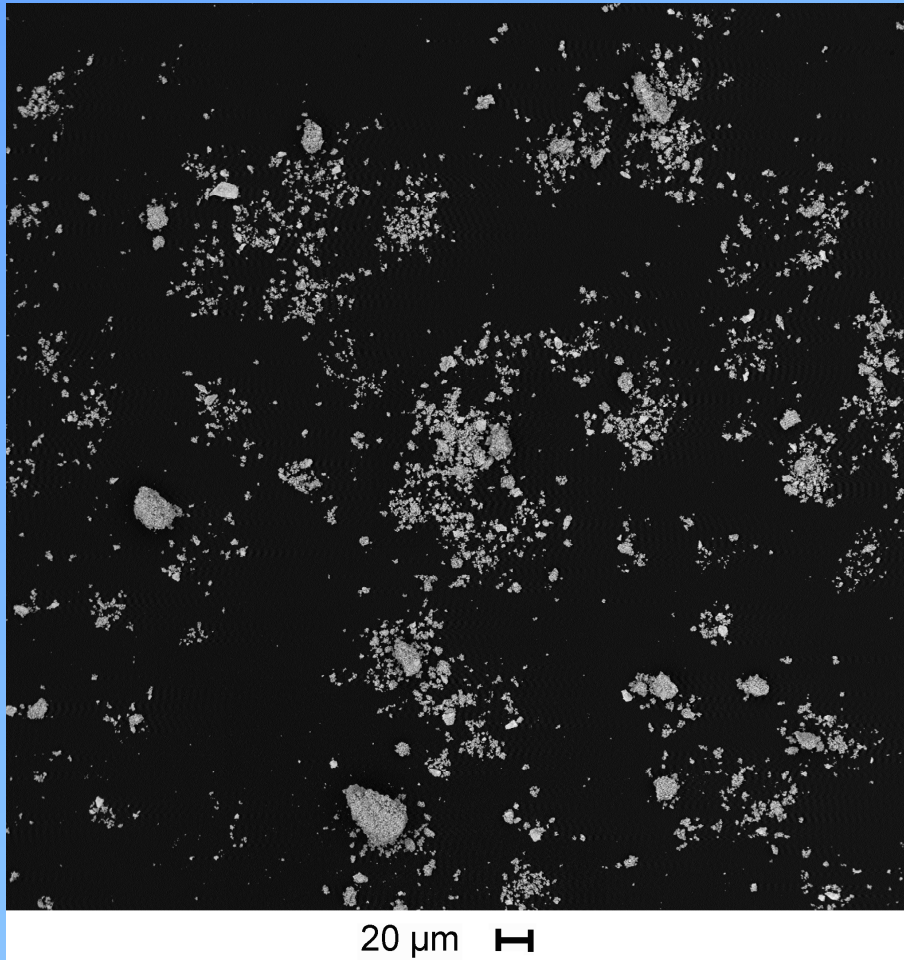
PLZT Results

Previous synthesis: variety of phase evolution paths and several intermediate compositions



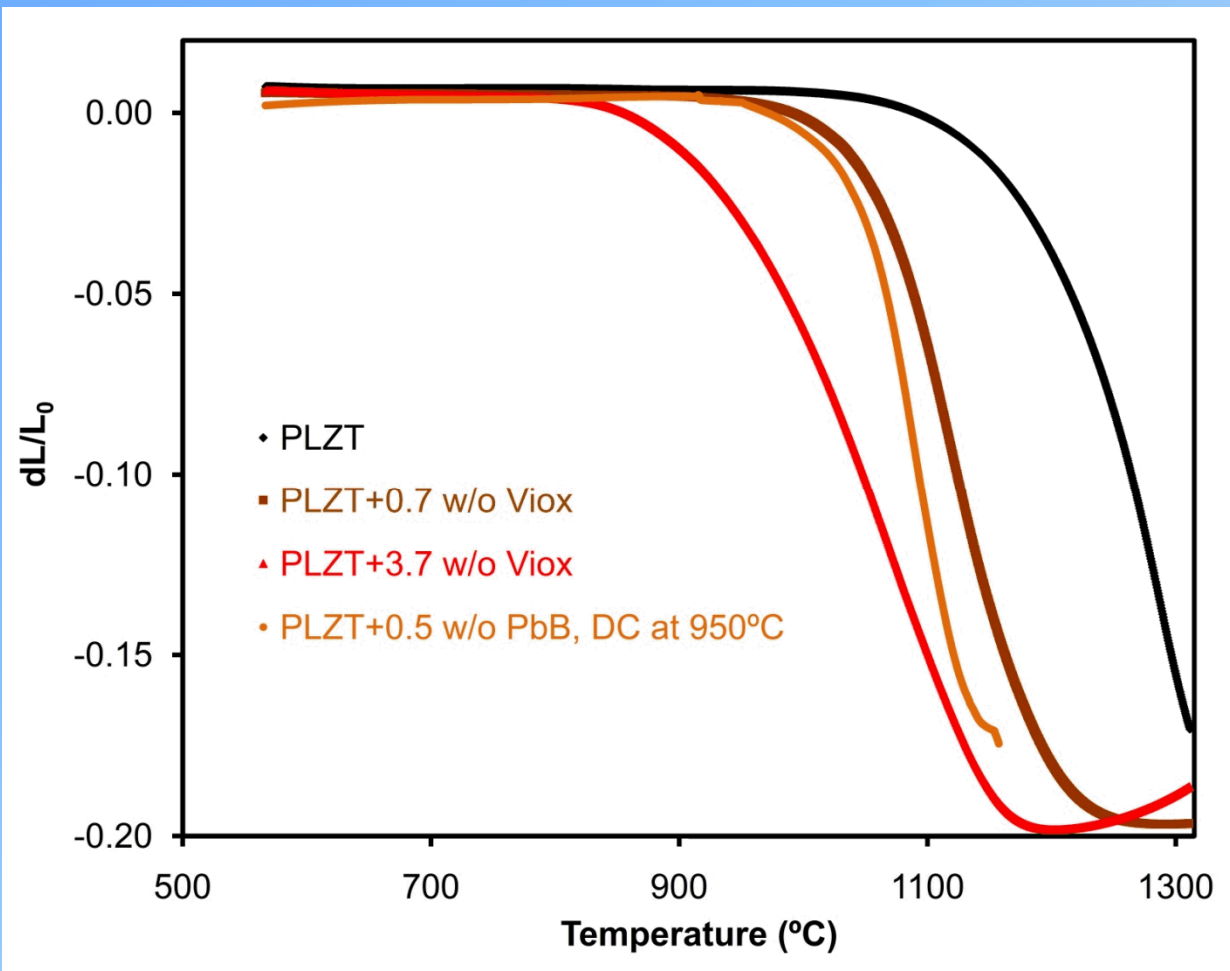
Full understanding of raw materials and better chemistry control allows simplification of the synthesis route

Large calcined particle size, nanoscale crystallite size



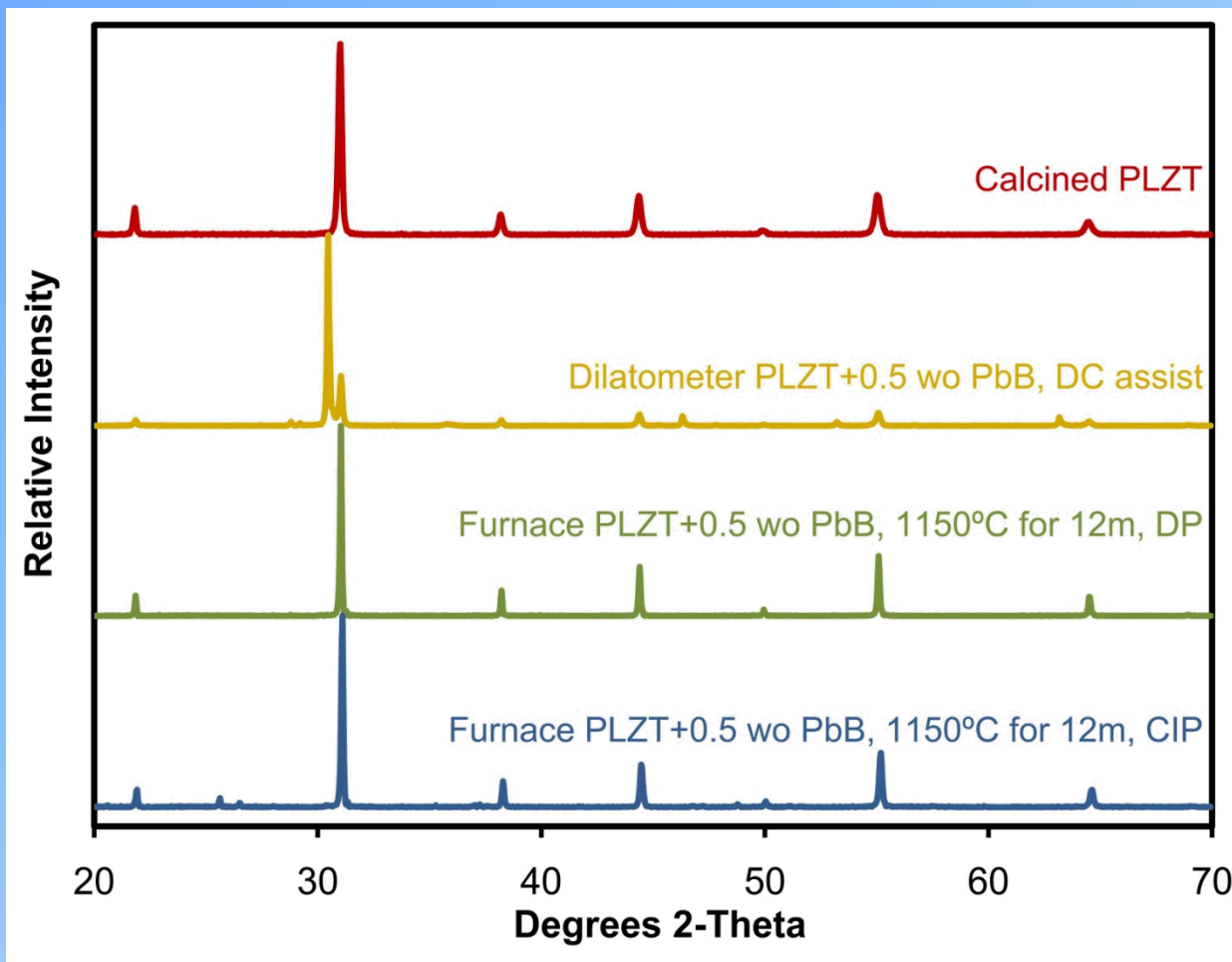
While this result was not anticipated, it may facilitate sample fabrication by easing safety issues

Choice of Glass Sintering Aids



- Several glass sintering aids are available
- Optimizing the chemistry and quantity is essential

Post-Sintering XRD



- Secondary surface phases are present after dilatometer sintering
 - Likely due to platinum reaction or uncontrolled atmosphere